分类号 ----------　　密级 ----------

U D C----------　　编号 ----------

中国科学院理论物理研究所

学 位 论 文

平面半导体微腔中的激子极化激元

李 定 洲

指导教师：　苏 肇 冰 研究员　中国科学院理论物理研究所

申请学位：　理学硕士　　专业：　理论物理

论文答辩日期：　1999 年 6 月 17 日

学位授予单位：　中国科学院理论物理研究所

学位授予日期：　1999 年　　月　　日

答辩委员会主席：　王 垂 林 研究员

评　　阅　　人：　王 炳 [illegible] 研究员

王 垂 林 研究员

Excitonic Polariton in Planar Semiconductor Microcavity

Dingzhou Li

Dissertation for Master degree of Science

Institute of Theoretical Physics, CAS
P.O. Box 2735, Beijing 100080
P.R. China

June 1999

摘 要

我们研究了平面半导体微腔中激子极化激元对光学响应的贡献。由于量子阱中空穴子带四分量之间有较强的耦合，以及量子阱生长方向的非局域性，计入以上效应之后，我们基于空穴四分量旋量的描述，推导出了介质极化传播子的具体形式。我们把这个电导率公式应用到具体的平面半导体微腔结构，该结构两端带有分布式布拉格反射器。我们发现 2p 激子也可以和光子耦合，形成所谓的极化激元。我们还讨论了和腔模耦合的不同旋量分量的“选择定则”。作为该方法的一个应用，在入射角超过一定值后，出现了另一套分裂的峰，这对应着轻空穴激子极化激元。激子极化激元具有内禀压缩性，我们计算了轻空穴和重空穴激子的压缩因子。

关键词： 激子 极化激元 空穴四分量旋量 内禀压缩

Acknowledgements

First I give the grateful thanks to my supervisors, Prof. Zhao-Bin Su and Prof. Bingshen Wang, who have given me kind help and instructed me a lot in the related fields during my two-year staying at ITP. Their personalities also affect me greatly. I also owe much to Dr. Gu Xu, our work cannot be completed without her painstaking calculations and collaboration. I am very appreciated for Dr. Jizhong Lou's help on computer programming and many technical issues. I would like to also thank Dr. Yuxi Liu, Dr. Congjun Wu, Dr. Xi Dai and Dr. Xiaoqing Yu for their constructive remarks and suggestions on my work. I would like to thank Sha Yang for her constant help and care. Finally I dedicate this paper to my beloved parents for their love and supports.

Abstract

The contribution of excitonic polariton to the optical response is studied in planar semiconductor microcavity (SMC). Considering the hybridization between the four components of the hole subband in quantum wells (QW) and the non-local effect along the growth direction of QW, we deduce the expression for the medium polarization propagator based on the 4-component spinor description for holes. We apply the conductivity to the detailed structure of SMC with distributed Bragger reflectors at two ends. We find that the 2p exciton can also couple to photon and form polariton. The "selection rule" for different spinor components of the exciton in coupling with cavity mode is discussed. As an application of this approach, we find also one another set of splitted peaks of the light hole exciton-polariton beyond certain incident angle. The excitonic polariton is found to be intrinsic squeezed. The squeezing factor is calculated for both light hole and heavy hole.

Contents

Chapter 1

Introduction

The theory of polariton has been greatly developed since the first work of Huang[1]. The strong coupling between elementary excitations and light make it difficult to use ordinary perturbation theory to treat optical process in such circumstance. Hopfield pointed out the exciton-light system in semiconductor is actually a kind of polariton[2]. A semiconductor microcavity (SMC) provides a good environment for observing such effect. There is only a single light mode that is dominant in the cavity under suitable boundary conditions. The strong-coupling regime can be easily achieved due to the interaction of the privileged mode and the exciton with the same momentum of photon (i.e. a result of translation invariance). Thus neither the interaction nor the final states of the system has a continous momentum distribution. In this case, Fermi's Golden Rule is no longer valid and we should solve the problem exactly.

Since the first experiment on the quantum well (QW) excitonic polariton in the semiconductor microcavity (SMC)[3] being reported, there appeared extensive experimental and theoretical studies[4] - [20] for the excitonic polaritons in QW's and multiple QW's embedded in SMC, even for the bulk[13] or quantum wire[9]excitonic polaritons in SMC. It is found under various physical conditions, such as with the presence of electric field, magnetic field and thermal factors, the excitonic polaritons in SMC display quite different properties from that of isolated QWs. It is clear in many experimental result such as stimulated emission[10] spetrum, Raman scattering[12], Zeeman effect[14] and ultrafast radiation[15]. However the existing study did not concern the realistic exciton structure seriously and some of these using simple dielectric model[21] originally developed for atom in microcavities.

It is known that, for the tetrahedral bulk semiconductors, the top of the valence band

for is four-fold degenerate. In the microstructure consisted of these materials, away from the Γ point of 2D wave wector plane (usualy the growth plan[100]), the coupling between the motion within the growth plane and the motion along the growth direction will mix all of the four components. Therefore the heavy hole(HH) and the light hole (LH) cannot be decoupled as in the bulk case, and the hole envelop function will aquire a 4-component spinor structure. This hybridization between HH and LH often plays a nontrivial role[23][24]. The coupling between exciton and the photon field becomes complex and some new coupling which does not exist in simple exciton models may appear. It has remarkable observable consequence on the energy level [25] and the selection rules for optical transitions of the excitons in QW[26][27]. Since the hole hybridization induced excitons are usually weak, it is interesting to investigate such effect for the exciton polariton of the QW embedded in a SMC, where the exciton-photon coupling could be enhanced a great deal. Although there has no such experiment been reported, it is generally believed that the quality of the distributed Bragg reflectors (DBR's) and SMC as well as the resolution for the experimental measurements will be improved substantially in the near future, we would like to study such interesting effect in advance.

In fact, the exciton-polariton is essentially a quantum many body effect and can be understood as a results of medium polarization. In case for the effect of hole subband hybridization, the effective coupling between photons and hybridization induced exciton can only be adequately calculated from dielectric response microscopically. Moreover, in calculation of exciton-polariton for the quantum wells, we have only translational invariance perpendicular to the growth direction, the non-local dielectric response along the growth direction should be carefully treated[22]. In particular, the barrier confinement effect with 4-component spinor-like hole wave function should appeared in the non-local dielectric response. To our knowledge, both those factors have not been considered in a serious way yet. Furthermore, the DBR is a periodic structure for the light propagation and is designed for the interested frequency which locates in the center of its (nearly) forbidden optical band. A pair of DBR's can play the role of mode selection for region confined by itself, so that they are highly sensitive and phase coherent optical devices. The light propagating in the SMC will not only be polarized by the QW medium but also coherently couple to the two neighboring DBR's via associated boundary conditions, i.e., the DBR-SMC(QW)-DBR system should be treated as a whole.

Based upon the above considerations, we would like to provide a self-consistent semiclassical description for the excitonic polaritons in QW embedded in SMC, in which the

hole subband hybridization, the nonlocality induced by the QW barrier confinement and the boundary conditions for the SMC in connection with the DBR's have all been consistently taken into account. The light is treated semiclassically but the medium polarization in QW is treated in the context of quantum many-body theory with the electromagnetic wave-electron-hole interaction, so that the description for the effective coupling between light and excitons does not need any phenomenological input "coupling constant". The only input parameters are the width for the exciton levels.

The calculated Rabi splitting for the conventional excitonic polaritons could be considered as an improvement to the dielectric model where the photon-exciton coupling constant is approximated through exciton oscillator strength from simple exciton model and electric field of the assumed single photon mode, and often estimated as empirical parameters. We will show also the complexity for introducing such effective oscillator strength due to the coupling of the motion along and perpendicular to the growth directions for the realistic exciton-polaritons. As an interesting effect of the barrier confinement induced electron's and hole's envelop wave functions for a system with a pair of symmetric DBR's, we apply the parity symmetry analysis along the growth direction to the symmetric DBR's and SMC confined QW, and obtain a sort of selection rule for the excitonic polaritons in the QW, which is also quite useful for searching the hole subband hybridization induced polaritons. We calculate an example for such polaritons and show some of its possible distinguished features for measurements. As a further application of this approach, we calculated the incident angle dependence of the LH induced polaritons. We find another set of weakly splitted peaks polaritons beyond certain value of the incident angle. We interpret it as a result of the coupling between exciton and perpendicular component electrical field induced p-polarized photon.

Polaritons are known to be intrinsic squeezed for a decade, which can display some nonclassical properties in number statistics and noise supression. Actually, to get the point, we need a two-step transformation: first, a simple mixing of photon and exciton, then a Bogoliugov transformation is carried out. So the "squeezing" is only respected to polaritons. However, an appropiate method to measure the squeezing and how to compare the theoretical results with experiments in SMC case are still to come, because we can only measure the output of a SMC which may alter the magnitude and property of squeezing inside. The double-photon term is essential to the origin of squeezing, though often negleted in current-current correlation. We note that we cannot use our Green function method to calculate the squeezing spectrum since we have already treated light as semiclassical. However, we expect

to modify the method to achieve the goal. At the present stage, we follow second-quantization procedure to just have an estimate of the polariton squeezing in SMC.

The paper is organized as the following. In chapter 2, a preliminary background about four-component description of excitons in QW is given. Chapter 3 is devoted to a quantum many-body description for the medium polarization in QW and its applications to the excitonic polariton in SMC. We also give an analysis about the parity symmetry and relative phase difference between each component which has important consequence on the selection rule of exciton-photon interaction. Finally in chapter 4, the Hamiltonian of exciton-photon system in SMC is formulated to show the squeezing properties of excitonic polariton and a calculation of squeezing factor is also presented.

Chapter 2

4-component description for excitons in semiconductor

In fact, in QWs the coupling between HH and LH would make significant modifications to both the quantative results and qualitive analysis, such as selection rule. Besides, the translation invariance along the growth direction is broken. The envelop function model which is the basis for studying the behaviour of exciton in such environment. But first we would like to have a brief review on the origin of heavy hole and light hole: spin-orbit coupling.

2.1 Spin-orbit coupling; heavy hole and light hole

At the bottom of conduction band in tetrahedral cystal, the cell function is Γ_1 representation of T_d group denoted as $|s\rangle$, while at the top of valence band, the cell functions are Γ_4 representation which are $|X\rangle$, $|Y\rangle$, $|Z\rangle$. So actually the orbital quantum number of conduction band electron is 0 (s state) and that of valence band eletron is $1(p$ state). Considering that the electron has it own spin quantum number, there exists the spin-orbit interaction:

$$H_{so} = \frac{\hbar}{4c^2m^2}(\nabla V \times \vec{p}) \cdot \vec{\sigma} \tag{2.1}$$

The eigenfunction of (2.1) are eigenstates of the total angular momentum j. So conduction eletron can be labeled as $|s\rangle|\alpha\rangle$ and $|s\rangle|\beta\rangle$ with total angular number $j_c = \frac{1}{2}$ where $|\alpha\rangle$ and $|\beta\rangle$ are spin-up and spin-down state, respectively. For valence band electron, j_v can take

two value:$\frac{1}{2}$ and $\frac{3}{2}$. However, we are only interested in $j_v = \frac{3}{2}$ states:

$$
\begin{aligned}
|3/2, 3/2\rangle &= -(|X\rangle + i|Y\rangle)|\alpha\rangle/\sqrt{2} \\
|3/2, 1/2\rangle &= -[(|X\rangle + i|Y\rangle)|\beta\rangle - 2|Z\rangle|\alpha\rangle]/\sqrt{6} \\
|3/2, -1/2\rangle &= [(|X\rangle - i|Y\rangle)|\beta\rangle + 2|Z\rangle|\alpha\rangle]/\sqrt{6} \\
|3/2, -3/2\rangle &= (|X\rangle - i|Y\rangle)|\alpha\rangle/\sqrt{2}
\end{aligned} \tag{2.2}
$$

the energy corresponding to $j_v = \frac{1}{2}$ states is greatly separated from conduction band bottom energy E_c and valence band top energy E_v, so we neglect those states when treating excitons.

$|3/2, 3/2\rangle$ and $|3/2, -3/2\rangle$ are called "heavy hole" because their effective mass is much bigger than that of $|3/2, 1/2\rangle$ and $|3/2, -1/2\rangle$ which are called "light hole". Anyway, when the coupling effect is pronounced as we will see later, we can no longer classify these two kinds of holes so easily.

2.2 Envelop function model and Luttinger Hamiltonian

In case that a perturbing potential(electric field, magnetic field, heterstructure-induced potential etc.) V_p is applied on the eletrons in semiconductor, the envelop function model is commonly used to describe the motion of electrons so long as the potential is slow-varying in space.

Schrödinger Equation is

$$(H_0 + V_p)\Psi_n(\vec{r}) = E_n\Psi_n(\vec{r}) \tag{2.3}$$

If the band is undegenaratd, e.g. at the bottom of conduction band, the wave function can be written as the product of envelop $\psi_n(\vec{r})$ and Bloch cell function $u_n(\vec{r})$:

$$\Psi_n(\vec{r}) = \psi_n(\vec{r})u_n(\vec{r}) \tag{2.4}$$

Substituting the above into Eq.(2.3) and using the $k \cdot p$ perturbation equation for $u_n(\vec{r})$, we have

$$(\frac{p^2}{2m*} + V_p)\psi_n(\vec{r}) = (E_n - E_c)\psi_n(\vec{r}) \tag{2.5}$$

$m*$ is effective mass.

If the band is degenerated, e.g. at the top of valence band, the wave function can be represented as the linear combination of the product of envelop function $\psi_{n,j}(\vec{r})$ and Bloch cell function $u_{n,j}(\vec{r})$:

$$\Psi_n(\vec{r}) = \sum_j \psi_{n,j}(\vec{r}) u_{n,j}(\vec{r}) \tag{2.6}$$

in which j can be a set of quantum numbers.

Then $\psi_{n,j}(\vec{r})$ can be proved to satisfy the following equation array

$$\sum_j D_{ij}^{\mu\nu} \frac{\partial}{\partial x_\mu} \frac{\partial}{\partial x_\nu} \psi_{n,j}(\vec{r}) + V_p \psi_{n,j}(\vec{r}) = (E_n - E_v)\psi_{n,i}(\vec{r}) \tag{2.7}$$

$D_{ij}^{\mu\nu}$ are called effective mass paremeters in which off-diagonal elements bear out both anisotropism and coupling between different branches. In this paper we make the approximation:

$$\begin{aligned} E_c &= E_g - \mu \\ E_v &= \mu \end{aligned} \tag{2.8}$$

E_g is the gap which separates the conduction band and the valence band, μ is the chemical potential

Now we would like to give the envelop equations for the GaAs like material. First it is necessary to introduce the meaning of each index if we want to have a more compact form of Hamiltonian. The Bloch cell function for the conduction band $u_\alpha^{(c)}(\vec{r})$ is a spin doublet with its index $\alpha = \frac{1}{2}, -\frac{1}{2}$, while that cell function for the valence band $u_{\alpha'}^{(v)}(\vec{r})$ can be taken as a four component spinor with $\alpha' = \frac{3}{2}, \frac{1}{2}, -\frac{1}{2}, -\frac{3}{2}$, the HH subband corresponds to $\alpha' = \pm\frac{3}{2}$, and the LH subband corresponds to $\alpha' = \pm\frac{1}{2}$. The plus and minus signs refer to time reversal (Kramer's)degenerated states. In the effective mass approximation, the non-interacting Hamiltonian for the envelop functions written in the first quantization representation has the form as

$$H^{(0)}_{\alpha,\alpha';\beta,\beta'} = H^e_{\alpha,\beta}\delta_{\alpha',\beta'} + \delta_{\alpha,\beta}H^h_{\alpha',\beta'} \tag{2.9}$$

$$H^e_{\alpha,\beta} = \delta_{\alpha,\beta}\Big[\frac{1}{2m^e_{\|}}\Big(\frac{\hbar}{i}\frac{\partial}{\partial \vec{r}_{\|,e}}\Big)^2 + \frac{1}{2m^e_{\perp}}\Big(\frac{\hbar}{i}\frac{\partial}{\partial z_e}\Big)^2 + Eg - \mu + V_e(\vec{r}_{\|,e}, z_e)\Big] \tag{2.10}$$

$$H^h_{\alpha',\beta'} = \frac{1}{2m}\begin{pmatrix} P_1, & Q, & R, & 0 \\ Q^*, & P_2, & 0, & R \\ R^*, & 0, & P_2, & -Q \\ 0, & R^*, & Q, & P_1 \end{pmatrix} + \delta_{\alpha',\beta'}(\mu + V_h^{(\alpha')}(\vec{r}_{\|,h}, z_h)) \tag{2.11}$$

where

$$
\begin{aligned}
P_1 &= (\gamma_1+\gamma_2)\Big(\tfrac{\hbar}{i}\tfrac{\partial}{\partial \vec{r}_{\|}}\Big)^2 + (\gamma_1-2\gamma_2)\Big(\tfrac{\hbar}{i}\tfrac{\partial}{\partial z_h}\Big)^2 \\
P_2 &= (\gamma_1-\gamma_2)\Big(\tfrac{\hbar}{i}\tfrac{\partial}{\partial \vec{r}_{\|}}\Big)^2 + (\gamma_1+2\gamma_2)\Big(\tfrac{\hbar}{i}\tfrac{\partial}{\partial z_h}\Big)^2 \\
Q &= -i2\sqrt{3}\gamma_3\Big(\tfrac{\hbar}{i}\tfrac{\partial}{\partial z_h}\Big)\Big(\Big(\tfrac{\hbar}{i}\tfrac{\partial}{\partial x_h}\Big) - i\Big(\tfrac{\hbar}{i}\tfrac{\partial}{\partial y_h}\Big)\Big) \\
R &= \sqrt{3}\Big[\gamma_2\Big(\Big(\tfrac{\hbar}{i}\tfrac{\partial}{\partial x_h}\Big)^2 - \Big(\tfrac{\hbar}{i}\tfrac{\partial}{\partial y_h}\Big)^2\Big) - 2i\gamma_3\Big(\tfrac{\hbar}{i}\tfrac{\partial}{\partial x_h}\Big)\Big(\tfrac{\hbar}{i}\tfrac{\partial}{\partial y_h}\Big)\Big]
\end{aligned}
\tag{2.12}
$$

In Eqs. (2.10)-(2.12), conduction electron coordinate $\vec{r}_e = (\vec{r}_{\|,e}, z_e)$ with $\vec{r}_{\|,e} = x_e\vec{e}_x + y_e\vec{e}_y$, the valence hole coordinate $\vec{r}_h = (\vec{r}_{\|}, z_h)$ with $\vec{r}_{\|,h} = x_h\vec{e}_x + y_h\vec{e}_y$; m is the physical electron mass, $m^e_\perp$ and $m^e_{\|}$ are effective masses of the conduction electrons corresponding to its moving direction perpendicular or parallel to the z-axis; V^e and V^h are the confinement potentials which form the barriers for the QW. For the DBR–SMC(QW)–DBR system interested in this paper, V_e and V_h are actually $\vec{r}_{\|,e}$ and $\vec{r}_{\|,h}$ independent. Eqs(2.11) and (2.12) is the well known Luttinger Hamiltonian[31]which is written down in a form with a specific choice of the coordinates. In these two equations, Q and R describe the hybridization between the HH subbands and the LH subbands, and $\gamma_1, \gamma_2, \gamma_3$ are band structure parameters. We notice that the envelop function description engaged in this paper is valid around the Γ point. We denote $\varphi^{(b,\lambda)}_{s,\alpha}(\vec{r})$ as the envelop function which can be solved from the eigenvalue equation for the Hamiltonian Eqs. (2.10) and (2.11) with appropriate boundary conditions in connection with the confinement barriers as follow:

$$
\sum_{\beta} H^e_{\alpha,\beta}\varphi^{(c,\lambda)}_{s,\beta}(\vec{r}) = \varepsilon^{(c,\lambda)}_s \varphi^{(c,\lambda)}_{s,\alpha}(\vec{r}) \tag{2.13}
$$

$$
\sum_{\beta'} H^h_{\alpha',\beta'}\varphi^{(v,\lambda)}_{s,\beta'}(\vec{r}) = \varepsilon^{(v,\lambda)}_s \varphi^{(v,\lambda)}_{s,\alpha'}(\vec{r}) \tag{2.14}
$$

Its correspondent energy eigenvalues are denoted as $\varepsilon^{(b,\lambda)}_s$. We call them as sub-energies. In these notations, $b = c$ refers to the conduction band with $\lambda = \pm\frac{1}{2}$ corresponding to a spin doublet; $b = v$ refers to the valence band with indices $\lambda = \pm\frac{1}{2}, \pm\frac{3}{2}$ which describe branches of valence band resuted from diagonalizing the hybridized Hamiltonian Eq. (2.11). Notice that each of the eigenfunctions(envelop functions) coresponding to these branch of valence band is a four component spinor. We again name the envelop functions with $\lambda = \pm\frac{3}{2}$ as the HH branch and that with $\lambda = \pm\frac{1}{2}$as the LH branch according to the properties that λ-spinor has the dominant component as $\alpha = \lambda$. Moreover, s is the quantum number depending on the confinement potential. It is discrete along the direction of confinement but continuous in the extended direction.

2.3 Exciton theory in QW with coupling effect

For an exciton which is an electron-hole pair (either bound state or extented state), the envelop function equation can be put as

$$\sum_{\beta,\beta'}\Big(H^{(0)}_{\alpha,\alpha';\beta,\beta'} - \delta_{\alpha,\beta}\delta_{\alpha',\beta'}\frac{e^2}{\varepsilon_c|\vec{r}_e-\vec{r}_h|}\Big)\psi^{(\lambda,s;\lambda',s';n)}_{\beta\beta'}(\vec{r}_e,\vec{r}_h) = E^{(\lambda,s;\lambda',s')}_n\psi^{(\lambda,s;\lambda',s';n)}_{\alpha\alpha'}(\vec{r}_e,\vec{r}_h) \tag{2.15}$$

in which the Coulumb interaction between electron and hole is included. $\psi^{(\lambda,s;\lambda',s';n)}_{\alpha\alpha'}(\vec{r}_e,\vec{r}_h)$ is the two body exciton-like wave function for the n-th eigenstate which is constituted by a conduction electron with quantum number λ, s in $(\vec{r}_e,\alpha)$ representation and a valence hole with quantum number λ', s' in $(\vec{r}_h,\alpha')$ representation. Of course it is only valid for the QW that is not very wide, otherwise the exciton could not be simply contructed from only one eletron sub-energy state s and one hole sub-energy state state s'. In that case several electron or hole sub-energy state with very close sub-energies will contribute to a single exciton because the difference between these sub-energies is much smaller than exciton bound energy in wide QW.

The general subband indices and quantum numbers "$\lambda, s; \lambda', s', n$" now are specified into the following set as "$\vec{q}_{\|}; n_{ex}, l; n, j_c; n', j_h$". $\vec{q}_{\|}$ is the 2D center of mass momentum for the exciton, which is a good quantum number describing the translational invariance in the X-Y plane for the system. n_{ex}, l are the quantum numbers for the eigenstate of the exciton describing the in plane relative motion for the virtual electron and hole pairs. n_{ex} is the major quantum number while l is the angular quantum number. n (n') is for the discrete states due to the confinement in the z-direction for the conduction electrons (valence holes), $j_c = \pm\frac{1}{2}$ is the subband indices describing the spin doublet for the conduction electron while $j_h = \pm\frac{1}{2}$, $\pm\frac{3}{2}$ is the subband indices for the valence holes with the meaning as the total angular momentum induced by spin-orbit coupling.

For solving $\psi^{(\vec{q}_{\|};n_{ex},l;n,j_c;n',j_h)}_{\alpha,\alpha'}(\vec{r}_e,\vec{r}_h)$ from Eq.(2.15), we need the complete set of eigen functions of the non-interacting Hamiltonian described by Eqs (2.10) and (2.11) for the conduction electron and valence hole respectively. We express them as

$$\frac{1}{\sqrt{L^2}}e^{i\vec{k}_{\|,e}\cdot\vec{r}_{\|,e}}\varphi^{(c)}_n(z_e)\delta_{j_c,\alpha} \tag{2.16}$$

for the conduction electrons and

$$\frac{1}{\sqrt{L^2}}e^{i\vec{k}_{\|,h}\cdot\vec{r}_{\|,h}}\varphi^{(v)}_{n',j_h;\alpha'}(\vec{k}_{\|,h};z_h) \tag{2.17}$$

for the valence holes with subband hybridization, where L^2 is the extension for the QW in X-Y plane in sense of quantization condition for the plane wave states. In solving Eqs. (2.10) and (2.11), there are an energy eigenvalue ϵ_n^cassociated with $\varphi_n^{(c)}(z_e)$ for the z-direction electronic motion and another eigenvalue $\epsilon_{n',j_h}^{(v)} = \epsilon_{n',j_h}^{(v)}(\vec{k}_{\|} = 0)$associated with the $\varphi_{n',j_h;\alpha'}^{(v)}(\vec{k}_{\|,h}, z_h)$ which could be also interpreted as for the z-direction hole motion. Actually, for the hole in valence band, the motion along the z-direction described by its eigen wave function $\varphi_{n',j_h;\alpha'}^{(v)}$ is coupled to its motion in the X-Y plane characterized by $\vec{k}_{\|,h}$. So $\varphi_{n',j_h;\alpha'}^{(v)}$ depends not only on z_h but also on $\vec{k}_{\|,h}$ meanwhile $\epsilon_{n',j_h}^{(v)}$ also has the $\vec{k}_{\|,h}$ dependence. Such a subtlety is due to the hybridization term Q and R in Eq. (2.11) and (2.12)

We notice further that, in the QW region $V_h^{(\alpha')}(\vec{r}_{\|,h}, z)$ is constant so that we choice it equal to zero, the z-axis parity symmetry changes its sign alternatively for the matrix elements of the Luttinger Hamiltonian Eq.(2.11) along its each row and each column. This interesting symmetry properties makes the hole eigenfunction for Eq.(2.11) has an amazing parity symmetry as that, the first and the third components ($\alpha' = \frac{3}{2}, -\frac{1}{2}$) have the same parity symmetry along z-axis but opposite to that of the other two components ($\alpha' = \frac{1}{2}, -\frac{3}{2}$). Moreover, since the Luttinger parameters γ_2 and γ_3 are usually rather close to each other, we may assume that they are equal as $\gamma_2 = \gamma_3$ (isotropic approximation in $X-Y$ plane). We further introduce a polar coordinate $(k_{\|,h}, \vartheta_h)$ for $\vec{k}_{\|,h}$ in the X-Y plane as $\vec{k}_{\|,h} = k_{\|,h}(\cos\vartheta_h\vec{e}_x + \sin\vartheta_h\vec{e}_y)$. Following Eq.(2.12), we would have $Q \sim e^{-i\vartheta_h}$ and $R \sim e^{-2i\vartheta_h}$. So the phase difference in $k_{\|,h}$ space between neighbouring components is ϑ_h. As a result, the corresponding eigenfunction in Eq.(2.17) will acquire the following functional dependence

$$\varphi_{n',j_h;\alpha'}^{(v)}(\vec{k}_{\|,h}, z_h) = e^{i(j_h-\alpha')\vartheta_h}\varphi_{n',j_h;\alpha'}^{(v)}(k_{\|,h}z_h) \tag{2.18}$$

in which ϑ_h being separated from $\varphi_{n',j_h;\alpha'}^{(v)}(k_{\|,h}z_h)$ and the product $k_{\|,h}z_h$ being a single dimensionless argument.

We then expand the two-body exciton like wave function in terms of the non-interacting electron and hole wave functions as Eqs. (2.16) and(2.17) for a fixed set of good quantum numbers $\vec{q}_{\|}; n_{ex}, l; n, j_c; n', j_h$ as

$$\begin{aligned}\psi_{\alpha,\alpha'}^{(\vec{q}_{\|};n_{ex},l;n,j_c;n',j_h)}(\vec{r}_e, \vec{r}_h) = \tfrac{1}{L^3}\textstyle\sum_{\vec{k}_{\|,e}}\sum_{\vec{k}_{\|,h}}\delta_{\vec{q}_{\|},\vec{k}_{\|,e}+\vec{k}_{\|,h}}e^{i(\vec{k}_{\|,e}\cdot\vec{r}_{\|,e}+\vec{k}_{\|,h}\cdot\vec{r}_{\|,h})}\cdot \\ f_{n_{ex},l}^{(n;n',j_h)}(\vec{k}_{\|,e}, \vec{k}_{\|,h})\cdot\varphi_n^{(c)}(z_e)\delta_{j_c,\alpha}\varphi_{n',j_h;\alpha'}^{(v)}(\vec{k}_{\|,h}, z_h)\end{aligned} \tag{2.19}$$

The expansion coefficient $f_{n_{ex},l}^{(n;n',j_h)}(\vec{k}_{\|,e}, \vec{k}_{\|,h})$ has the physical meaning as the 2D excitonic wave function for which the center of mass degree of freedom has been separated. If we

ignore the hybridization terms Q and R in the hole Hamiltonian Eq. (2.11), and further ignore the z_e, z_h dependence for the coulomb interaction in Eq.(2.15) as the thickness of the QW is rather small, we can show easily that the $f_{n_{ex},l}^{(n;n',j_h)}(\vec{k}_{\|,e}, \vec{k}_{\|,h})$would be precisely the 2D hydrogen atom solution of Eq.(2.15) constrained by $\vec{q}_{\|} = \vec{k}_{\|,e} + \vec{k}_{\|,h}$. Since now we have the hybridization, the physical meaning for $f_{n_{ex},l}^{(n;n',j_h)}(\vec{k}_{\|,e}, \vec{k}_{\|,h})$ is no more so transparent. It should be determined by substituting itself into Eq. (2.15).

Chapter 3

Effect of the complex valence band structure on the excitonic polariton in planar semiconductor microcavity

In Sec.1, we show the expression for the medium polarization propagator with both positive- and negative frequency parts, which is applicable for the generic non-translational invariant systems. In Sec.2, by summing over the degenerated states due to Kramer's and space inversion symmetries, we show the detailed expression for the nonlocal conductivity tensor which is proved to be diagonal and can be factorized into a sum of bi-products. It makes its non-locality effect to be explicit. In Sec.3, we formulate the description for the excitonic polaritons in QW embedded in a SMC in terms of a propagating electromagnetic field, while the SMC is further confined by a pair of DBR's. The basic spirit of its classical electrodynamic aspect for such a description is mainly following [28]. One of the crucial difference is that the physics contained in the formal expression for the dielectric response. Literature [28] is mainly for the inter-conduction-subband transition and no coulomb interaction and complexity of the valence band involved, while that of ours is devoted to the inter-band transition particularly for the hybridization effect of the hole band. In Sec.4, we present our results and discussions.

3.1 Non-local polarization propagator of quasi 2-D exciton

It is known that the conductivity tensor is connected to the medium polarization tensor as

$$\sigma(\omega;\vec{r},\vec{r}') = \frac{i}{\omega}\pi_r(\omega;\vec{r},\vec{r}) \tag{3.1}$$

Intuitively, in the light propagation, the dominant contribution to the medium polarization should be the virtual excitations ofelectron-hole pairs. For clarifying certain conceptual problems, we would like to discuss such an ideal situation: the intrinsic state of the QW at low temperature, i.e., the valence band is almost fully filled while the conduction band is almost fully empty. Then the virtual pairs are constituted by conduction electrons and valence holes. For such a case, the Coulomb interaction should induce a series of exciton states distributed in the semiconductor gap. They are bound states or extended states formed by conduction electrons and valence holes. These virtual bounded $e-h$ pairs should also contribute to the medium polarization even at zero temperature for an intrinsic QW. Based upon such an understanding, the medium polarization can be calculated straightforwardly. We notice that there are no requirement for the spatial translational invariance, so that it can be applied to any sort of QW's. It also leads such an advantage, i.e., if apply it to the planar QW, the in-plane center of mass momentum for the excitons can be explicitly treated which is a non-trivial property for the excitonic polaritons.

Now we are going to deduce the exact form of the media polarization tensor by a summation over the Coulomb interacting ladder diagrams accommodated in a bubble diagram constituted by a conduction electron and a valence hole as shown in Fig.3.1. The upper and lower series of diagram correspnd to positive frequency and negative frequency respectively, which stand for two opposite propagations.

We introduce the second quantized wave operator and the second quantized current operator:

$$\hat{\psi}(\vec{r}) = \sum_b \sum_\lambda \sum_s \sum_\alpha \varphi_{s,\alpha}^{(b,\lambda)}(\vec{r}) u_\alpha^{(b)}(\vec{r}) \hat{c}_s^{(b,\lambda)} \tag{3.2}$$

$$\hat{\vec{j}}(\vec{r}) = \frac{e\hbar}{2imc}(\hat{\psi}^\dagger(\vec{r})\nabla\hat{\psi}^\dagger(\vec{r}) - \nabla\hat{\psi}^\dagger(\vec{r})\hat{\psi}(\vec{r})) \tag{3.3}$$

in which $\varphi_{s,\alpha}^{(b,\lambda)}(\vec{r})$ is the eigen wavefunction of non-interacting Hamiltonian as Eq.(2.13) and (2.14), $u_\alpha^{(b)}(\vec{r})$ is Bloch cell function and $\hat{c}_s^{(b,\lambda)}$ is the second quantized electron annihilation

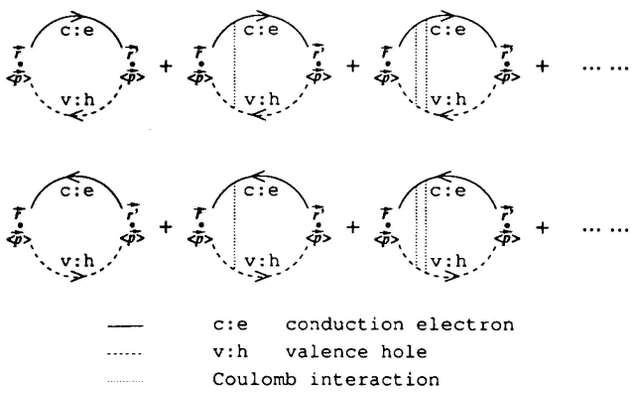

Figure 3.1: The summed coulumb interacting electron-hole bubble diagram series for the medium polarization

operator for state with band index c, λ and quantum number s, note that we dropped the index k of the cell-periodic functions of Bloch function, this corresponds to the envelop function approximation: ignoring cell-periodic function's change with k and using the corresponding at the band extrema. Using the approximation of linear response theory and Mastubara representation, the polarization part of the electron system $\pi_r(\omega;\vec{r},\vec{r}')$ can be expressed as

$$\pi_r(\omega;\vec{r},\vec{r}') = -\int_0^\infty d\tau e^{i\omega_n\tau} Tr\{\hat{\rho}T_\tau \hat{\vec{j}}(\vec{r},\tau)\hat{\vec{j}}(\vec{r}',0)\}|_{i\omega_n\to\omega+i\eta} \tag{3.4}$$

where $\hat{\rho}$ is the thermal density matrix and Tr is the trace operation, T_τ is the chronological operation along the imaginary time axis. Expression (3.4) have the advantage that it can be calculated systematically by applying the diagrammatical technique. We notice first that, for each pair of electron and hole lines in the upper series of diagrams in Fig. 3.1, it contributes a term as

$$\frac{1-n(\xi_s^{(c,\lambda)})-n(\xi_{\bar{s}'}^{(v,\lambda')})}{i\omega_n-\xi_s^{(c,\lambda)}-\xi_{\bar{s}'}^{(v,\lambda')}}$$

$\bar{s}'$ describes the quantum numbers charge conjugated to s' (i.e. the annihilation of an electron in the valence band corresponds to the creation of a hole with opposite momentum and spin). But for each pair of electron and hole lines in the lower series of diagrams in Fig. 3.1 with their arrow directions reversed, it contributes a term as

$$-\frac{1-n(\xi_s^{(c,\lambda)})-n(\xi_{\bar{s}'}^{(v,\lambda')})}{i\omega_n+\xi_s^{(c,\lambda)}+\xi_{\bar{s}'}^{(v,\lambda')}} \tag{3.6}$$

in which $\xi_s^{(c,\lambda)} = \varepsilon_s^{(c,\lambda)} + E_g - \mu$ and $\xi_s^{(v,\lambda)} = \varepsilon_s^{(v,\lambda)} + \mu$ and $n(\xi)$ is the Fermi distribution function for the conduction electrons and valenceholes. Moreover, a dotted Coulomb line contributes a factor

$$v_{s',s'';s',s'''}^{\lambda,\lambda'';\lambda',\lambda'''} = \sum_{\alpha,\alpha'} \int d^3r d^3r' \varphi_{s,\alpha}^{*(c,\lambda)}(\vec{r}) \varphi_{s'',\alpha}^{(c,\lambda'')}(\vec{r}) \frac{1}{\varepsilon_c |\vec{r} - \vec{r}'|} \varphi_{s',\alpha'}^{*(v,\lambda')}(\vec{r}') \varphi_{s''',\alpha'''}^{(v,\lambda''')}(\vec{r}') \tag{3.7}$$

where $\varepsilon_c = \varepsilon_c(\omega)$ is the background dielectric constant for the medium. Finally, each vertex at the end point of the bubble contributes a dipole matrix elements $\langle c, \alpha | \vec{p} | v, \alpha' \rangle$ or $\langle v, \alpha' | \vec{p} | c, \alpha \rangle$.

$$\langle c, \alpha | \vec{p} | v, \alpha' \rangle \equiv \frac{1}{\Omega} \int_\Omega d^3r \frac{\hbar}{2i} (u_\alpha^{*(c)}(\vec{r}) \nabla u_{\alpha'}^{(v)}(\vec{r}) - \nabla u_\alpha^{*(c)}(\vec{r}) \cdot u_{\alpha'}^{(v)}(\vec{r})) \tag{3.8}$$

All the above expressions follow straightforwardly from the quantum many-body text-book with an additional considering exhibitted in(3.2), i.e. our basis wave function is not simple plane wave as usual, but the envelop function associated with a more "microscopic" cell periodic function u.

It should also be noticed that, for intrinsic semiconductor under low excitation limit, the conduction band are almost completely empty and the valence band are almost completely full, so the two Fermi distribution functions in Eqs. (3.5) and (3.6) can be taking as zero. Furthermore this guarantees that only the ladder diagrams contribute, because any self-energy term for either the electron or the hole contain closed loops which are proportional to the density of particles.[34].

The first diagram in the series is that for no interaction:

$$\begin{aligned} \pi^{(0)}(i\omega_n; \vec{r}, \vec{r}') = \quad & \left(\frac{e}{m}\right)^2 \sum_{\alpha,\alpha'} \sum_{\alpha'',\alpha'''} \sum_{\lambda,s} \sum_{\lambda',s'} \Big\{ \varphi_{s,\alpha}^{(c,\lambda)}(\vec{r}) \varphi_{s',\alpha'}^{*(v,\lambda')}(\vec{r}) \langle v, \alpha' | \vec{p} | c, \alpha \rangle \\ & \cdot \frac{1}{i\omega_n - \xi_s^{(c,\lambda)} - \xi_{\bar{s}'}^{(v,\lambda')}} \varphi_{s,\alpha''}^{*(c,\lambda)}(\vec{r}') \varphi_{s',\alpha'''}^{(v,\lambda')}(\vec{r}') \langle c, \alpha'' | \vec{p}' | v, \alpha''' \rangle \\ & - \varphi_{s,\alpha}^{*(c,\lambda)}(\vec{r}) \varphi_{s',\alpha'}^{(v,\lambda')}(\vec{r}) \langle c, \alpha | \vec{p} | v, \alpha' \rangle \\ & \cdot \frac{1}{i\omega_n + \xi_s^{(c,\lambda)} + \xi_{\bar{s}'}^{(v,\lambda')}} \varphi_{s,\alpha''}^{(c,\lambda)}(\vec{r}') \varphi_{\bar{s}',\alpha'''}^{*(v,\lambda')}(\vec{r}') \langle v, \alpha''' | \vec{p}' | c, \alpha'' \rangle \Big\} \end{aligned} \tag{3.9}$$

The second ladder diagram with one dotted Coulomb line has the form

$$\pi^{(1)}(i\omega_n;\vec{r},\vec{r}') = -\Big(\frac{e^2}{m}\Big)^2 \sum_{\alpha,\alpha'}\sum_{\alpha'',\alpha'''}\sum_{\lambda,s}\sum_{\lambda',s'}\sum_{\lambda'',s''}\sum_{\lambda''',s'''}\Big\{\varphi^{(c,\lambda)}_{s,\alpha}(\vec{r})\varphi^{*(v,\lambda''')}_{s''',\alpha'''}(\vec{r})\langle v,\alpha'''|\vec{p}|c,\alpha\rangle$$
$$\cdot\frac{1}{(i\omega_n-\xi^{(c,\lambda)}_{s}-\xi^{(v,\lambda')}_{\bar{s}'})}\frac{1}{(i\omega_n-\xi^{(c,\lambda'')}_{s}-\xi^{(v,\lambda''')}_{\bar{s}'''})}v^{\lambda,\lambda'';\lambda''',\lambda'}_{s,s'';s''',s'}\varphi^{*(c,\lambda'')}_{s,\alpha''}(\vec{r}')\varphi^{(v,\lambda')}_{s',\alpha'}(\vec{r}')\langle c,\alpha''|\vec{p}'|v,\alpha'\rangle$$
$$-\varphi^{*(c,\lambda)}_{s,\alpha}(\vec{r})\varphi^{(v,\lambda''')}_{s''',\alpha'''}(\vec{r})\langle c,\alpha|\vec{p}|v,\alpha'''\rangle$$
$$\cdot\frac{1}{(i\omega_n+\xi^{(c,\lambda)}_{s}+\xi^{(v,\lambda')}_{\bar{s}'})}\frac{1}{(i\omega_n+\xi^{(c,\lambda'')}_{s}+\xi^{(v,\lambda''')}_{\bar{s}'''})}v^{\lambda'',\lambda;\lambda',\lambda'''}_{s'',s;s',s'''}\varphi^{(c,\lambda'')}_{s,\alpha''}(\vec{r}')\varphi^{*(v,\lambda')}_{s',\alpha'}(\vec{r}')\langle v,\alpha'|\vec{p}'|c,\alpha''\rangle\Big\} \tag{3.10}$$

Accordingly, we can get the form of each $\pi^{(n)}(i\omega_n;\vec{r},\vec{r}')$ but it is a rather lengthy expression. Through summation over the Coulomb interacting ladder diagrams accommodated in a bubble diagram constituted by a conduction electron and a valence hole as shown in Fig. 3.1, we can obtain following expression for the polarization tensor,

$$\begin{aligned}\pi(i\omega_n;\vec{r},\vec{r}') = \;& \pi^{(0)}(i\omega_n;\vec{r},\vec{r}')+\pi^{(1)}(i\omega_n;\vec{r},\vec{r}')+\pi^{(2)}(i\omega_n;\vec{r},\vec{r}')+\cdots\\ = \;& \Big(\frac{e}{m}\Big)^2\sum_{\alpha,\alpha'}\sum_{\lambda,s}\sum_{\lambda',s'}\Big\{\varphi^{(c,\lambda)}_{s,\alpha}(\vec{r})\varphi^{*(v,\lambda')}_{s',\alpha'}(\vec{r})\langle v,\alpha'|\vec{p}|c,\alpha\rangle\\ & \cdot\frac{1}{i\omega_n-\xi^{(c,\lambda)}_{s}-\xi^{(v,\lambda')}_{\bar{s}'}}\Gamma^{\lambda,\lambda'}_{s,s'}(i\omega_n;\vec{r}')\\ & -\varphi^{*(c,\lambda)}_{s,\alpha}(\vec{r})\varphi^{(v,\lambda')}_{s',\alpha'}(\vec{r})\langle c,\alpha|\vec{p}|v,\alpha'\rangle\\ & \cdot\frac{1}{i\omega_n+\xi^{(c,\lambda)}_{s}+\xi^{(v,\lambda')}_{\bar{s}'}}\tilde{\Gamma}^{\lambda,\lambda'}_{s,s'}(i\omega_n;\vec{r}')\Big\}\end{aligned} \tag{3.11}$$

$$\begin{aligned}\Gamma^{\lambda,\lambda'}_{s,s'}(i\omega_n;\vec{r}') = \;& \textstyle\sum_{\alpha'',\alpha'''}\varphi^{*(c,\lambda)}_{s,\alpha''}(\vec{r}')\varphi^{(v,\lambda')}_{s',\alpha'''}(\vec{r}')\langle c,\alpha''|\vec{p}'|v,\alpha'''\rangle\\ & +(-e^2)\textstyle\sum_{\lambda'',s''}\sum_{\lambda''',s'''}v^{\lambda,\lambda'';\lambda''',\lambda'}_{s,s'';s''',s'}\cdot\\ & \cdot\frac{1}{i\omega_n-\xi^{(c,\lambda'')}_{s''}-\xi^{(v,\lambda''')}_{\bar{s}'''}}\Gamma^{(\lambda'',\lambda''')}_{s'',s'''}(i\omega_n;\vec{r}')\end{aligned} \tag{3.12}$$

$$\begin{aligned}\tilde{\Gamma}^{\lambda,\lambda'}_{s,s'}(i\omega_n;\vec{r}') = \;& \textstyle\sum_{\alpha'',\alpha'''}\varphi^{(c,\lambda)}_{s,\alpha''}(\vec{r}')\varphi^{*(v,\lambda')}_{\bar{s}',\alpha'''}(\vec{r}')\langle v,\alpha'''|\vec{p}'|c,\alpha''\rangle\\ & -(-e^2)\textstyle\sum_{\lambda'',s''}\sum_{\lambda''',s'''}v^{\lambda'',\lambda;\lambda',\lambda'''}_{s'',s;s',s'''}\\ & \cdot\frac{1}{i\omega_n+\xi^{(c,\lambda'')}_{s''}+\xi^{(v,\lambda''')}_{\bar{s}'''}}\tilde{\Gamma}^{\lambda'',\lambda'''}_{s'',s'''}(i\omega_n;\vec{r}')\end{aligned} \tag{3.13}$$

we then introduce two auxiliary functions as

$$\begin{aligned}P_{\alpha,\alpha'}(i\omega_n;\vec{\tilde{r}},\vec{\tilde{r}}';\vec{r}') = \;& \textstyle\sum_{\tilde{\lambda},\tilde{s}}\sum_{\tilde{\lambda}',\tilde{s}'}\varphi^{(c,\tilde{\lambda})}_{\tilde{s},\alpha}(\vec{\tilde{r}}')\varphi^{*(v,\tilde{\lambda}')}_{\tilde{s}',\alpha'}(\vec{\tilde{r}}')\\ & \frac{1}{i\omega_n-\xi^{(c,\tilde{\lambda})}_{\tilde{s}}-\xi^{(v,\tilde{\lambda}')}_{\tilde{s}'}}\Gamma^{(\tilde{\lambda},\tilde{\lambda}')}_{\tilde{s},\tilde{s}'}(i\omega_n;\vec{r}')\end{aligned} \tag{3.14}$$

and

$$\tilde{P}_{\alpha,\alpha'}(i\omega_n;\vec{\vec{r}},\vec{\vec{r}}';\vec{r}') = \sum_{\tilde{\lambda},\tilde{s}}\sum_{\tilde{\lambda}',\tilde{s}'}\varphi^{*(c,\tilde{\lambda})}_{\tilde{s},\alpha}(\vec{\vec{r}})\varphi^{(v,\tilde{\lambda}')}_{\tilde{s}',\alpha'}(\vec{\vec{r}}') \frac{1)}{i\omega_n+\xi^{(c,\tilde{\lambda})}_{\tilde{s}}+\xi^{(v,\tilde{\lambda}')}_{\tilde{s}'}}\tilde{\Gamma}^{(\tilde{\lambda},\tilde{\lambda}')}_{\tilde{s},\tilde{s}'}(i\omega_n;\vec{r}') \tag{3.15}$$

By substituting (3.14) into (3.12) together with (3.7), we get

$$\begin{aligned}\Gamma^{\lambda,\lambda'}_{s,s'}(i\omega_n;\vec{r}') = \sum_{\alpha,\alpha'}\{&\varphi^{*(c,\lambda)}_{s,\alpha}(\vec{r}')\varphi^{(v,\lambda')}_{s',\alpha'}(\vec{r}')\langle c,\alpha|\vec{p}'|v,\alpha'\rangle \\ &+(-e^2)\int d^3r_1 d^3r_2\varphi^{*(c,\lambda)}_{s,\alpha}(\vec{r_1})\tfrac{1}{\varepsilon_c|\vec{r_1}-\vec{r_2}|}\varphi^{(v,\lambda')}_{s',\alpha'}(\vec{r_2})P_{\alpha,\alpha'}(i\omega_n;\vec{\vec{r}}_2,\vec{\vec{r}}_1;\vec{r}')\}\end{aligned} \tag{3.16}$$

and the similar form holds for $\tilde{\Gamma}^{\lambda,\lambda'}_{s,s'}(i\omega_n;\vec{r}')$

From Eq(3.11), (3.14) and (3.15) , the polarization tensor can now be derived into

$$\begin{aligned}\pi(i\omega_n;\vec{r},\vec{r}') = \left(\tfrac{e}{m}\right)^2\sum_{\alpha,\alpha'}\{&\langle v,\alpha'|\vec{p}|c,\alpha\rangle P_{\alpha,\alpha'}(i\omega_n;\vec{r},\vec{r};\vec{r}') \\ &-\langle c,\alpha|\vec{p}|v,\alpha'\rangle\tilde{P}_{\alpha,\alpha'}(i\omega_n;\vec{r},\vec{r};\vec{r}')\}\end{aligned} \tag{3.17}$$

Next, we operate the operator $i\omega_n\delta_{\alpha,\alpha''}\delta_{\alpha',\alpha'''}-[H_0]_{\alpha,\alpha';\alpha'',\alpha'''}$ to the $P_{\alpha'',\alpha'''}(i\omega_n;\vec{\vec{r}},\vec{\vec{r}}';\vec{r}')$ from the left. By recalling (2.13) and (2.14) we have

$$\begin{aligned}\Big\{i\omega_m\delta_{\alpha,\alpha''}\delta_{\alpha',\alpha'''} - \Big(H_0\Big[\vec{\vec{r}},\tfrac{1}{i}\tfrac{\partial}{\partial\vec{\vec{r}}};\vec{\vec{r}}',\tfrac{1}{i}\tfrac{\partial}{\partial\vec{\vec{r}}'}\Big]\Big)_{\alpha,\alpha';\alpha'',\alpha'''}\Big\}P_{\alpha'',\alpha'''}(i\omega_m;\vec{\vec{r}},\vec{\vec{r}}';\vec{r}') \\ = \sum_{\lambda,s}\sum_{\lambda',s'}\varphi^{(c,\lambda)}_{s,\alpha''}(\vec{\vec{r}})\varphi^{*(v,\lambda')}_{s',\alpha'''}(\vec{\vec{r}}')\Gamma^{\lambda,\lambda'}_{s,s'}(i\omega_n;\vec{r}')\end{aligned} \tag{3.18}$$

Again, we substitute (3.16) into the right side of (3.18) to get an equation solely for the auxiliary function

$$\begin{aligned}\Big\{i\omega_m\delta_{\alpha,\alpha''}\delta_{\alpha',\alpha'''} - \Big(H_0\Big[\vec{\vec{r}},\tfrac{1}{i}\tfrac{\partial}{\partial\vec{\vec{r}}};\vec{\vec{r}}',\tfrac{1}{i}\tfrac{\partial}{\partial\vec{\vec{r}}'}\Big]\Big)_{\alpha,\alpha';\alpha'',\alpha'''}\Big\}P_{\alpha'',\alpha'''}(i\omega_m;\vec{\vec{r}},\vec{\vec{r}}';\vec{r}') \\ = \sum_{\lambda,s}\sum_{\lambda',s'}\sum_{\beta,\beta'}\Big[\varphi^{(c,\lambda)}_{s,\alpha''}(\vec{\vec{r}}')\varphi^{*(v,\lambda')}_{s',\alpha'''}(\vec{\vec{r}}')\varphi^{*(c,\lambda)}_{s,\beta}(\vec{r}')\varphi^{(v,\lambda')}_{s',\beta'}(\vec{r}')\langle c,\beta|\vec{p}|v,\beta'\rangle \\ +(-e^2)\varphi^{(c,\lambda)}_{s,\alpha''}(\vec{\vec{r}})\varphi^{*(v,\lambda)}_{s,\alpha''}(\vec{\vec{r}}')\cdot \\ \int d^3r_1 d^3r_2\varphi^{*(c,\lambda)}_{s,\beta}(\vec{r_1})\tfrac{1}{\varepsilon_c|\vec{r_1}-\vec{r_2}|}\varphi^{(v,\lambda')}_{s',\beta'}(\vec{r_2})P_{\beta,\beta'}(i\omega_n;\vec{\vec{r}}_2,\vec{\vec{r}}_1;\vec{r}')\Big]\end{aligned} \tag{3.19}$$

By utilizing the completeness relation for $\varphi^{(c,\lambda)}_{s,\alpha}(\vec{r})$ and $\varphi^{(v,\lambda')}_{s',\alpha'}(\vec{r}')$ the above equation turns into

$$\begin{aligned}\Big\{i\omega_m\delta_{\alpha,\alpha''}\delta_{\alpha',\alpha'''} - \Big(H_0\Big[\vec{\vec{r}},\tfrac{1}{i}\tfrac{\partial}{\partial\vec{\vec{r}}};\vec{\vec{r}}',\tfrac{1}{i}\tfrac{\partial}{\partial\vec{\vec{r}}'}\Big] - e^2\tfrac{1}{|\vec{\vec{r}}-\vec{\vec{r}}'|}\Big)_{\alpha,\alpha';\alpha'',\alpha'''}\Big\} \\ P_{\alpha'',\alpha'''}(i\omega_m;\vec{\vec{r}},\vec{\vec{r}}';\vec{r}') = \langle c,\alpha|\vec{p}|v,\alpha'\rangle\delta(\vec{\vec{r}}-\vec{r}')\delta(\vec{\vec{r}}'-\vec{r}')\end{aligned} \tag{3.20}$$

Likewise, we find the equation for $\tilde{P}_{\alpha'',\alpha'''}(i\omega_m;\vec{\vec{r}},\vec{\vec{r}}';\vec{r}')$ noting that $i\omega_n\delta_{\alpha'',\alpha}\delta_{\alpha''',\alpha'}+[H_0]_{\alpha'',\alpha''';\alpha,\alpha'}$ is operated to the right of $\tilde{P}_{\alpha'',\alpha'''}(i\omega_m;\vec{\vec{r}},\vec{\vec{r}}';\vec{r}')$

$$\sum_{\alpha''}\sum_{\alpha'''}\tilde{P}_{\alpha'',\alpha'''}(i\omega_m;\vec{\tilde{r}},\vec{\tilde{r}}';\vec{r}')\Big\{i\omega_m\delta_{\alpha'',\alpha}\delta_{\alpha''',\alpha'}+\Big(H_0\Big[\vec{\tilde{r}},\tfrac{1}{i}\tfrac{VC\partial}{\partial\vec{\tilde{r}}};\vec{\tilde{r}}',\tfrac{1}{i}\tfrac{\partial}{\partial\vec{\tilde{r}}'}\Big] -\tfrac{e^2}{|\vec{\tilde{r}}-\vec{\tilde{r}}'|}\Big)_{\alpha'',\alpha''';\alpha,\alpha'}\Big\}=\langle v,\alpha'|\vec{p}|c,\alpha\rangle\delta(\vec{\tilde{r}}-\vec{r}')\delta(\vec{\tilde{r}}'-\vec{r}') \tag{3.21}$$

We may then solve the auxiliary functions from Eqs. (and (soleP by Green's function method as

$$P_{\alpha,\alpha'}(i\omega_m;\vec{r},\vec{r};\vec{r}')=\sum_{\beta,\beta'}G_{\alpha,\alpha';\beta,\beta'}(i\omega_m;\vec{r},\vec{r};\vec{r}'\vec{r}')\langle c,\beta|\vec{p}|v,\beta'\rangle \tag{3.22}$$

$G_{\alpha,\alpha';\beta,\beta'}(i\omega_m;\vec{\tilde{r}},\vec{\tilde{r}}';\vec{r},\vec{r}')$ satisfies

$$\Big\{i\omega_m\delta_{\alpha,\beta}\delta_{\alpha',\beta'}-\Big(H_0\Big[\vec{\tilde{r}},\tfrac{1}{i}\tfrac{\partial}{\partial\vec{\tilde{r}}};\vec{\tilde{r}}',\tfrac{1}{i}\tfrac{\partial}{\partial\vec{\tilde{r}}'}\Big]-e^2\tfrac{1}{|\vec{\tilde{r}}-\vec{\tilde{r}}'|}\Big)_{\alpha,\beta;\alpha',\beta'}\Big\}$$
$$G_{\alpha'',\alpha''';\beta,\beta'}(i\omega_m;\vec{\tilde{r}},\vec{\tilde{r}}';\vec{r},\vec{r}')=\delta(\vec{\tilde{r}}-\vec{r}')\delta(\vec{\tilde{r}}'-\vec{r}') \tag{3.23}$$

With the aid of Hamiltonian equation (2.15) we can easily have

$$G_{\alpha'',\alpha''';\beta,\beta'}(i\omega_m;\vec{\tilde{r}},\vec{\tilde{r}}';\vec{r},\vec{r}')=\sum_{\lambda,s}\sum_{\lambda',s'}\sum_{n}\frac{\psi^{(\lambda,s;\lambda',s';n)}_{\alpha'',\alpha'''}(\vec{\tilde{r}},\vec{\tilde{r}}')\psi^{*(\lambda,s;\lambda',s';n)}_{\beta,\beta'}(\vec{r},\vec{r}')}{i\omega_m-E_n^{(\lambda,s;\lambda',s')}} \tag{3.24}$$

In the similar fashion, we get

$$\tilde{P}_{\alpha,\alpha'}(i\omega_m;\vec{r},\vec{r};\vec{r}')=\sum_{\beta,\beta'}\langle v,\beta'|\vec{p}|c,\beta\rangle\tilde{G}_{\beta,\beta';\alpha,\alpha'}(i\omega_m;\vec{r}',\vec{r}';\vec{r},\vec{r}) \tag{3.25}$$

with

$$\tilde{G}_{\beta,\beta';\alpha'',\alpha'''}(i\omega_m;\vec{r},\vec{r}';\vec{\tilde{r}},\vec{\tilde{r}}')=\sum_{\lambda,s}\sum_{\lambda',s'}\sum_{n}\frac{\psi^{(\lambda,s;\lambda',s';n)}_{\beta,\beta'}(\vec{r},\vec{r}')\psi^{*(\lambda,s;\lambda',s';n)}_{\alpha'',\alpha'''}(\vec{\tilde{r}},\vec{\tilde{r}}')}{i\omega_m+E_n^{(\lambda,s;\lambda',s')}} \tag{3.26}$$

By substituting Eqs. (3.22)-(3.26) into Eq.(3.17) and analytical continuation $i\omega\rightarrow\omega+i\eta$, we obtain the retard polarization tensor as follow:

$$\begin{aligned}\pi_r(\omega;\vec{r},\vec{r}')=\ &\Big(\tfrac{e}{m}\Big)^2\sum_{\alpha}\sum_{\alpha'}\sum_{\beta}\sum_{\beta'}\langle v,\alpha'|\vec{p}|c,\alpha\rangle\langle c,\beta|\vec{p}|v,\alpha\rangle\cdot\\ &\sum_{\lambda,s}\sum_{\lambda',s'}\sum_{n}\Big\{\frac{\psi^{(\lambda,s;\lambda',s';n)}_{\alpha\alpha'}(\vec{r},\vec{r})\psi^{*(\lambda,s;\lambda',s';n)}_{\beta\beta'}(\vec{r}',\vec{r}')}{\omega+i\eta-E_n^{(\lambda,s;\lambda',s';n)}}\\ &-\frac{\psi^{(\lambda,s;\lambda',s';n)}_{\alpha\alpha'}(\vec{r}',\vec{r}')\psi^{*(\lambda,s;\lambda',s';n)}_{\beta\beta'}(\vec{r},\vec{r})}{\omega+i\eta+E_n^{(\lambda,s;\lambda',s';n)}}\Big\}\end{aligned} \tag{3.27}$$

In Eq.(3.27) the exciton-like two body wave functions take value at $\vec{r}_e=\vec{r}_h=\vec{r}$ means that only those values of such wave functions can contribute to the spectral weight of polarization propagator, at which the electron meets the hole at the same spatial point. Moreover, the

first term in the bracket of Eq. (3.27) is its positive frequency part while the second is the negative frequency part. Both part are necessary for a boson-like propagator. We notice that the $\vec{r}$ and $\vec{r}'$ change into each other in the two correspondent spectral weights. We understand such a result that the positive frequency part corresponding to a sort of forward propagation while the negative frequency corresponding a sort of backward propagation. Only due to certain sort of existing symmetries for the system under investigation, the two spectral weight functions will equal to each other. This is one of the main topics for the next section.

We notice that, the $\psi_{\alpha\alpha'}^{(\lambda,s;\lambda',s';n)}(\vec{r}_e,\vec{r}_h)$ might not necessarily be the bound states only, the extended eigenstates of Eq.(2.15) should also contribute, since it is off-resonances for our interested frequency, it is attributed to the background dielectric constants.

3.2 Summation over the Degenerated States due to Space-Time Inversion Symmetries

After performing a summation over the space-time reversal transformationconnected degenerated states, we show in this subsection not only the positive and negativefrequency parts in the polarization propagator can be combined into one term, but also the non-diagonal elements for the polarizationtensor will also be canceled to be zero. This will make its expression to be neat and further simplify the calculation a great deal.

Actually what we needed for the spectral weight function in Eq.(3.27) is for the case of $\vec{r}_e = \vec{r}_h = \vec{r}$, so that, following Eq.(2.19), we have

$$\psi_{\alpha,\alpha'}^{(\vec{q}_{\|};n_{ex},l;n,j_c;n',j_h)}(\vec{r},\vec{r}) = \frac{1}{\sqrt{L^2}} e^{i\vec{q}_{\|}\cdot\vec{r}_{\|}} \delta_{j_c,\alpha} \frac{1}{L^2} \sum_{\vec{k}_{\|,e}} \sum_{\vec{k}_{\|,h}} \delta_{\vec{q}_{\|},\vec{k}_{\|,e}+\vec{k}_{\|,h}} \cdot f_{n_{ex},l}^{(n;n',j_h)}(\vec{k}_{\|,e},\vec{k}_{\|,h}) \varphi_n^{(c)}(z) \varphi_{n',j_h;\alpha'}^{(v)}(\vec{k}_{\|,h},z) \tag{3.28}$$

Moreover, the GaAs system has an energy gap $\sim$ 1.5 Ev. The wave length for the interested light has the order of magnitude$\sim 10^3$Å. On the other hand, the effective Bohr radius for the 2D-excitonin GaAs has the order of magnitude $\sim 10^2$Å. Therefore, $\vec{k}_{\|,e}$ and $\vec{k}_{\|,h}$ will span a region in the momentum space, in which the 2D excitonic wave function$f_{n_{ex},l}^{(n;n',j_h)}(\vec{k}_{\|,e},\vec{k}_{\|,h})$ has non-negligible contributions, much bigger than that of $\vec{q}_{\|}$. We may reasonably set $\vec{q}_{\|} \sim 0$ in the double summation for the $\vec{k}_{\|,e}$ and $\vec{k}_{\|,h}$, i.e., we may have approximately $\vec{k}_{\|,h} \cong -\vec{k}_{\|,e} = \vec{k}_{\|}$

in Eq.(3.28) within the double summation. Then

$$\begin{aligned}&\psi^{(\vec{q}_{\|};n_{ex},l;n,j_c;n',j_h)}(\vec{r},\vec{r})\\&=\frac{1}{\sqrt{L^2}}e^{i\vec{q}_{\|}\cdot\vec{r}_{\|}}\delta_{j_c,\alpha}\int\frac{d\vec{k}_{\|}}{(2\pi)^2}f^{(n;n',j_h)}_{n_{ex},l}(\vec{k}_{\|})\varphi^{(c)}_{n}(z)\varphi^{(v)}_{n',j_h;\alpha'}(\vec{k}_{\|},z)\end{aligned}\tag{3.29}$$

Intuitively, the 2D exciton-like wave function should have the expression as

$$f^{(n;n',j_h)}_{n_{ex},l}(\vec{k}_{\|})=f^{(n;n',j_h)}_{n_{ex},l}(k_{\|})e^{il\vartheta}\tag{3.30}$$

where $(k_{\|},\vartheta)$ is the polar coordinates for $\vec{k}_{\|}$. Then, by further utilizing Eq.2.18 and $\int_0^{2\pi}d\vartheta\exp i(l+j_h-\alpha')\vartheta=2\pi\delta_{l+j_h,\alpha}$, we obtain

$$\begin{aligned}&\psi^{(\vec{q}_{\|};n_{ex},l;n,j_c;n',j_h)}_{\alpha,\alpha'}(\vec{r},\vec{r})\\&=\frac{1}{\sqrt{L^2}}e^{i\vec{q}_{\|}\cdot\vec{r}_{\|}}\delta_{j_c,\alpha}\delta_{j_h+l,\alpha'}\int_0^{\infty}\frac{k_{\|}dk_{\|}}{2\pi}f^{(n;n',j_h)}_{n_{ex},l}(k_{\|})\end{aligned}\tag{3.31}$$

We substitute expression (3.31) into Eq.(3.27) with its indices changedfrom the general form into the present, and obtain

$$\begin{aligned}\pi_{r;\mu,\nu}(\omega;\vec{r},\vec{r}')=\frac{e^2}{m^2}\frac{1}{L^2}\sum_{\vec{q}_{\|}}\sum_{n_{ex},l}\sum_{n,j_c}\sum_{n',j_h},&j_h+l|p_{\mu}|c,j_c\rangle\langle c,j_c|p_{\nu}|v,j_h+l\rangle\\&\int_0^{\infty}\frac{k_{\|}dk_{\|}}{2\pi}\int_0^{\infty}\frac{k'_{\|}dk'_{\|}}{2\pi}f^{(n;n',j_h)}_{n_{ex},l}(k_{\|})f^{(n;n',j_h)}_{n_{ex},l}(k'_{\|})\\&\varphi^{(c)}_{n}(z)\varphi^{(c)}_{n}(z')\varphi^{(v)}_{n',j_h;\alpha'=j_h+l}(k_{\|}z)\cdot\varphi^{(v)}_{n',j_h;\alpha'=j_h+l}(k'_{\|}z')\\&\cdot\Big(e^{i\vec{q}_{\|}\cdot(\vec{r}_{\|}-\vec{r}'_{\|})}\frac{1}{\omega+i\eta-E^{(n;n',j_h)}_{n_{ex},l}(q_{\|})}-e^{-i\vec{q}_{\|}\cdot(\vec{r}_{\|}-\vec{r}'_{\|})}\frac{1}{\omega+i\eta+E^{(n;n',j_h)}_{n_{ex},l}(q_{\|})}\Big)\end{aligned}\tag{3.32}$$

where

$$E^{(n;n',j_d)}_{n_{ex},l}(q_{\|})=E_g+\epsilon^{(n;n',j_h)}_{q_{\|}}+\epsilon^{(n;n',j_h)}_{n_{ex},l}+\epsilon^{(c)}_{n}+\epsilon^{(v)}_{n',j_h}\tag{3.33}$$

which depends on $q_{\|}=|\vec{q}_{\|}|$ only. In Eq. (37), $\epsilon^{(n;n',j_h)}_{q_{\|}}$ is the kinetic energy for the center of mass of the 2D exciton and $\epsilon^{(n;n',j_h)}_{n_{ex},l}\leq 0$ is its bound energy; the $\epsilon^{(c)}_{n}$ and $\epsilon^{(v)}_{n'}$ are associated with the confinement potential for the conduction electrons and valence holes which has been introduced in connection with Eqs. (2.16) and (2.17). As mentioned several times, practically, due to the hybridization for the valence holes, it is difficult to separate $E^{(n;n',j_d)}_{n_{ex},l}(q_{\|})$ into such a neat form as in Eq.(3.33) with conventional interpretations. Expression (2.19) is essentially to be used as a variational wave function for the eigenvalue problem of Eq.(2.15) which can solved either approximately or numerically.

Besides the dynamical calculations, we have various symmetry properties for the system which are exact. Due to the space-time reversal symmetry, $E^{(n;n',j_d)}_{n_{ex},l}(q_{\|})$ and $f^{(n;n',j_d)}_{n_{ex},l}(k_{\|})$ are

degenerated with respect to $\pm l$, $j_c = \pm\frac{1}{2}$, $j_h = \pm\frac{1}{2}$ and $j_h = \pm\frac{3}{2}$. We have also the time reversal symmetry property for the hole wave function as

$$\varphi^{(v)}_{n',j_h;\alpha'}(z) = \varphi^{(v)}_{n',-j_h;-\alpha'}(z) \tag{3.34}$$

as further as that all the $f^{(n;n',j_h)}_{n_{ex},l}(k_\parallel)$, $\varphi^{(c)}_n(z)$ and $\varphi^{(v)}_{n,j_d;\alpha'}(k_\parallel z)$ are real functions. On the other hand, it is known that there is only one independent matrix element for $\langle v,\alpha'|p_\mu|c,\alpha\rangle$ as $p = \langle X|p_x|s\rangle = \langle Y|p_y|s\rangle = \langle Z|p_z|s\rangle$ where $\langle X|$, $\langle Y|$, $\langle Z|$ are orbital part of Bloch cell function for the hole band with $l = 1$ and $|s\rangle$ is the orbital part of the Bloch cell function for the conduction band. By making use of the Kramer's degeneracy properties and further the Clebsch-Gordon coefficients for the matrix elements $\langle v,\alpha'|p_\mu|c,\alpha\rangle$, we can sum over the plus and minus value of l, j_z and j_h but keep the absolute value for l, j_c, j_h and the correspondent energy eigenvalue to be fixed. After a lengthy calculations, the conductivity tensor in association with Eqs. (3.1) and (3.32) can be derived in a diagonal form as

$$\sigma_{\mu\nu}(\omega;\vec{r},\vec{r}\,') = \frac{1}{L^2}\sum_{\vec{q}_\parallel} e^{i\vec{q}_\parallel\cdot(\vec{r}_\parallel-\vec{r}\,'_\parallel)}\sigma_{\mu\nu}(\omega;\vec{q}_\parallel;z,z') \tag{3.35}$$

with

$$\begin{aligned}\sigma_{\mu\nu}(\omega;\vec{q}_\parallel;z,z') = {} & \tfrac{i}{\omega}\tfrac{e^2p^2}{m^2}\delta_{\mu,\nu}\textstyle\sum_n\sum_{n',j_h}\sum_{n_{ex},l}\sum_{l_h} \\ & P^{(n;n',j_h)}_{n_{ex},l}(\omega,q_\parallel)\cdot\phi^{(n;n',j_h)}_{n_{ex},l,l_h}(z)\eta^{(j_h;l,l_h)}_\mu\phi^{*(n;n',j_h)}_{n_{ex},l,l_h}(z')\end{aligned} \tag{3.36}$$

in which

$$\phi^{(n;n',j_h)}_{n_{ex},l,l_h}(z) = \int_0^\infty \frac{k_\parallel dk_\parallel}{2\pi} f^{(n;n',j_h)}_{n_{ex},l}(k_\parallel)\varphi^{(c)}_n(z)\varphi^{(v)}_{n',j_h;\alpha'=j_h+l_h}(k_\parallel z) \tag{3.37}$$

$$P^{(n;n',j_h)}_{n_{ex},l} = \frac{2E^{(n;n',j_h)}_{n_{ex},l}(q_\parallel)}{(\omega+i\gamma^{(n;n',j_h)}_{n_{ex},l})^2 - [E^{(n;n',j_h)}_{n_{ex},l}(q_\parallel)]^2} \tag{3.38}$$

In Eqs. (3.36),(3.37) and (3.38), j_h takes value of $\frac{3}{2}, \frac{1}{2}$ for HH and LH bands respectively, l takes value of 0 and 1. $l_h = 0$ if $l = 0$, whilel_h should be summed over ±1 if $l = 1$. This "new" quantum number l_h is resulted from the summation over the degenerated states due to Kramer's and space inversion symmetries. $\eta^{(j_h;l,l_h)}_\mu$ comes from the Clebsch-Gordoncoefficients for the dipole matrix elements with

$$\eta^{(3/2,0,0)}_\mu = \eta^{(1/2,1,1)}_\mu = 2\begin{pmatrix}|\langle X|3/2,3/2\rangle|^2\\ |\langle Z|3/2,3/2\rangle|^2\end{pmatrix} = \begin{pmatrix}1\\0\end{pmatrix}$$

$$\eta^{(1/2,0,0)}_\mu = \eta^{(3/2,1,1)}_\mu = \eta^{(1/2,1,-1)}_\mu = 2\begin{pmatrix}|\langle X|3/2,1/2\rangle|^2\\ |\langle Z|3/2,1/2\rangle|^2\end{pmatrix} = \begin{pmatrix}\frac{1}{3}\\ \frac{4}{3}\end{pmatrix}$$

$$\eta_{\mu}^{(3/2,1,1)} = 0 \tag{3.39}$$

where the upper component corresponds to the in-plane direction (x or y axis), while the down component corresponds to the growth direction (z axis). We stress that if we ignore the hybridization between the HH and LH subbands, then we have only $l = 0$ exciton states contribute to the spectral weight function. Meanwhile $\varphi^{(v)}_{n',j_h;\alpha'=j_h}(k_{\|}z)$ becomes $\varphi^{(v)}_{n',j_h;\alpha'=j_h}(z)$ being independent on$k_{\|}$. Therefore, the hole subbands hybridization induced excitonic polaritons are characterized by the angular quantum number as $l \neq 0$. We stress further that, in Eqs. (3.36) and (3.38), we replace $\omega + i\eta$ by $\omega + i\gamma^{(n;n',j_h)}_{n_{ex},l}$ in which $\gamma^{(n;n',j_h)}_{n_{ex},l}$ are the only phenomenological parameters introduced in this approach for describing the width of the exciton level.

3.3 Description for the Quantum Well in Cavity Confined by Distributed Bragg Reflectors

The semiconductor microcavity (SMC) under consideration consists of a quantum well (QW) of thickness Λ embedded in a thin layer semiconductor material which is sandwiched between a pair of distributed Bragg reflectors (DBR'S). This semiconductor layer serves as the barrier for the electrons and holes in QW meanwhile forms an optical cavity confined by the DBR's. The whole structure is schematically illustrated in Fig.3.2.

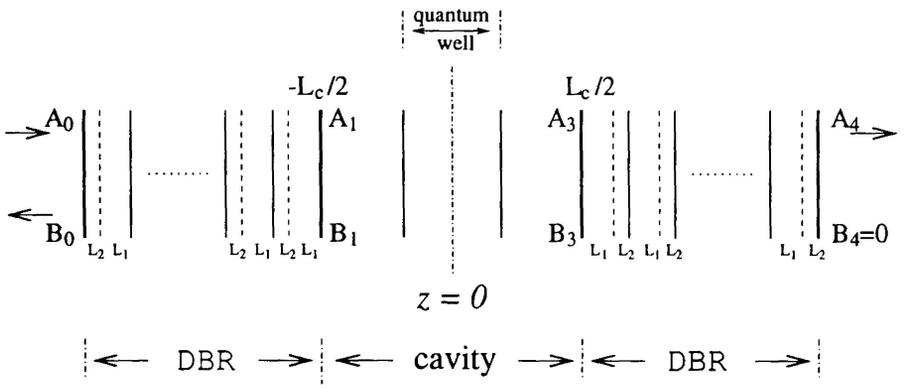

Figure 3.2: The schematic structure of the symmetric planer semiconductor microcavity

The thickness of the cavity is L_c with $\varepsilon_c(\omega)$ as its medium dielectric constant, where ω is the light frequency. We assume that theQW medium has the (backgroud) dielectric

constants same as that of the cavitymedium. The left (right) DBR is constructed from N_L (N_R)pairs of two alternating layers. One of the two layers has thelength as L_1 and dielectric constant as $\varepsilon_1(\omega)$ while the others has L_2 and $\varepsilon_2(\omega)$ respectively. We choose the z-axis as the growth direction with $z = 0$ being thecenter of the system. Therefore, QW is located at $(-\frac{\Lambda}{2}, \frac{\Lambda}{2})$ and the SMC occupies a region from $-\frac{L_c}{2}$ to $\frac{L_c}{2}$ with$L_c \geq \Lambda$. Consequently, $-\frac{L_c}{2}$ ($\frac{L_c}{2}$) is the boundary between the left (right) DBR and the SMC. Moreover, we rotate the coordinate axis aroundthe z-axis in such a way to make the incident light propagating in the $x - z$ plane. Then the wave vector has the form as $\vec{q} = (q_x \equiv q_{||},\ 0,\ q_z \equiv q_\perp)$ with q_y being always equal to zero. As a result, for the p-polarized wave, the electric field has only $x-$ and $z-$ components E_x and E_z, while for the s-polarized wave, the electric field has only y-component E_y. For a propagating wave with fixed frequency and $\vec{q}_{||} = q_{||}\vec{e}_x$ (where $\vec{e}_\mu,\ \mu = x, y, z$ is the unit vector along the μ-axis), its electric field has the form as

$$\vec{E}(\vec{r}, t) = \vec{E}(\omega, \vec{q}_{||}, z)e^{i(q_{||}x - \omega t)} = \vec{E}(\omega, \vec{r})e^{-i\omega t}. \tag{3.40}$$

The Maxwell equation for the electric field can be written as

$$\left[I\left(\nabla^2 + \frac{\omega^2}{c^2}\varepsilon_i(\omega)\right) - \vec{\nabla}\vec{\nabla}\right] \cdot \vec{E}(\omega, \vec{r}) = -\frac{4\pi i\omega}{c^2}\vec{j}(\omega, \vec{r}) \tag{3.41}$$

in which "i" is the medium index. Taking into consideration of Eg.(3.40), Eq.(3.41) can be simplified into

$$L_i(\omega, \vec{q}_{||}) \cdot \vec{E}(\omega, \vec{q}_{||}, z) = -\frac{4\pi i\omega}{c^2}\vec{j}(\omega, \vec{q}_{||}z) \tag{3.42}$$

with

$$L_i(\omega, \vec{q}_{||}) = I\Big(\frac{\partial^2}{\partial z^2} - q_{||}^2 + \frac{\omega^2}{c^2}q_i(\omega)\Big) - \Big(i\vec{q}_{||} + \vec{e}_z\frac{\partial}{\partial z}\Big)\Big(i\vec{q}_{||} + \vec{e}_z\frac{\partial}{\partial z}\Big) \tag{3.43}$$

For reason of simplicity, from now on, we discuss mainly the p-polarized wave propagation. It is straightforward to convert thediscussions for p-polarized wave into those for s-polarized wave. We will do it whenever necessary. Outside the QW medium, the polarization current density$\vec{j}(\omega, \vec{q}_{||}, z) = 0$ in Eq. (3.42). We then have plane wave solutions with $_{\perp,i} = \left[\frac{\omega^2}{c^2}\varepsilon_i(\omega) - q_{||}^2\right]^{1/2}$(3.43)For the left DBR, denoting the x-component of the incident and reflected amplitudes of the electric field as A_0 and B_0, which is defined by approaching from left to the left boundary of the left DBR. By applying the method of [29], we obtain the corresponding electric field amplitude as A_1 and B_1 at the right boundary of the left DBR which is also defined by approaching the boundary from the left as

$$\begin{pmatrix} A_0 \\ B_0 \end{pmatrix} = \begin{pmatrix} T_{11}^L, & T_{12}^L \\ T_{21}^L, & T_{22}^L \end{pmatrix} \begin{pmatrix} A_1 \\ B_1 \end{pmatrix} \tag{3.44}$$

with

$$\begin{pmatrix} T_{11}^L, & T_{12}^L \\ T_{21}^L, & T_{22}^L \end{pmatrix} = \begin{pmatrix} t_{11}^L, & t_{12}^L \\ t_{21}^L, & t_{22}^L \end{pmatrix}^{N_L} \tag{3.45}$$

Then for the right DBR, we introduce further A_3 and B_3. They are the forward (along the z-direction) and backward (reversed to the z direction) amplitudes of electric field respectively. They are defined by approaching from right to the left boundary of the right DBR. Meanwhile A_4 and B_4 are the corespondent amplitudesat the right boundary of the right DBR which is also defined by approaching the boundary from the right. We can similarly define the transfer matrix by solving the homogeneous Maxwell equations [29] and obtain

$$\begin{pmatrix} A_3 \\ B_3 \end{pmatrix} = \begin{pmatrix} T_{11}^R, & T_{12}^R \\ T_{21}^R, & T_{22}^R \end{pmatrix} \begin{pmatrix} A_4 \\ B_4 \end{pmatrix} \tag{3.46}$$

with

$$\begin{pmatrix} T_{11}^L, & T_{12}^R \\ T_{21}^R, & T_{22}^R \end{pmatrix} = \begin{pmatrix} t_{11}^R, & t_{12}^R \\ t_{21}^R, & t_{22}^R \end{pmatrix}^{N_R} \tag{3.47}$$

The detailed expressions for the matrix elements $t_{i,j}^L$ and t_{ij}^R with $i,j = 1,2$ are shown in Appendix . the QW region, there is a sort of additional medium polarization effect other than those described by its background dielectric constant. This is because that the virtual electron-hole pairscreation and annihilation processes will renormalize the light propagation in the QW region. In particular, the Coulomb interaction between the virtual electron-hole pairs may play crucial role in certain frequency range. In this section, we just introduce formally a conductivity tensor $\sigma(\omega, \vec{q}_{||}; z, z')$ to describe such an effect as

$$\vec{j}(\omega, \vec{q}_{||}, z) = \int dz' \sigma(\omega, \vec{q}_{||}; z, z') \cdot \vec{E}(\omega, \vec{q}_{||}, z') \tag{3.48}$$

which will be further investigated in the next section. Therefore, in the SMC region (including the QW), the Maxwell equation Eqs.(3.42) and (3.43) can be converted into an integral equation as

$$\begin{aligned} \vec{E}(\omega, \vec{q}_{||}; z) = \; & \vec{E}^{(c)}(\omega, \vec{q}_{||}; z) - \tfrac{4\pi i\omega}{c^2} \textstyle\int_{-\Lambda/2}^{\Lambda/2} dz' \int_{-\Lambda/2}^{\Lambda/2} dz'' G(\omega, \vec{q}_{||}; z, z') \cdot \\ & \sigma(\omega, \vec{q}_{||}; z', z'') \cdot \vec{E}(\omega, \vec{q}_{||}, z'') \end{aligned} \tag{3.49}$$

in which

$$\vec{E}^{(c)}(\omega, \vec{q}_{||}; z) = (A_c e^{iq_{\perp,c}z} + B_c e^{-iq_{\perp,c}z})\vec{e}_x - \frac{q_{||}}{q_{\perp,c}}(A_c e^{iq_{\perp,c}z} - B_c e^{-iq_{\perp,c}z})\vec{e}_z \tag{3.50}$$

is the homogeneous solution of Eq.(3.42), while $G(\omega, \vec{q}_{||}; z, z')$ is the Green's function[30]for theequation

$$L(\omega, \vec{q}_{||}) \cdot G(\omega, \vec{q}_{||}; z, z') = \delta(z - z') \tag{3.51}$$

We can easily solve Eq.(3.51) up to a homogeneous solution ofitself with its explicit expression. We notice that, in all equations: from Eq.(3.49)to Eq.(3.51), z and z' are confined in the region

$$-\frac{L_c}{2} \leq z \leq \frac{L_c}{2} \tag{3.52}$$

Moreover, the integral equation (3.49) exhibits the nonlocality not only provided by the Green's functions, but also induced by the medium polarization effect which is described by the conductivity tensor. To solve this integral equation, we emphasize that it should be solved with proper boundary conditions (BC). This is because that neither the homogeneous solution $\vec{E}^{(c)}(\omega, \vec{q}_{||}, z)$ nor the Green's functions are solved with respect to the correct BC's for the SMC. Therefore, following classical electrodynamics, we should have the BC at $z = \pm\frac{L_c}{2}$ as

$$\begin{aligned} A_1 + B_1 &= A_c e^{-iq_{\perp,c}\frac{L_c}{2}} + B_c e^{iq_{\perp,c}\frac{L_c}{2}} \\ &- \tfrac{4\pi i\omega}{c^2} \textstyle\sum_{\nu'=x,z} \sum_{\nu''=x,z} \int_{-\Lambda/2}^{\Lambda/2} dz' \int_{-\Lambda/2}^{\Lambda/2} dz'' G_{x,\nu'}\left(\omega, \vec{q}_{||}; -\tfrac{L_c}{2}, z'\right) \\ &\times \sigma_{\nu',\nu''}(\omega, \vec{q}_{||}; z', z'') E_{\nu''}(\omega, \vec{q}_{||}; z'') \end{aligned} \tag{3.53}$$

$$\begin{aligned} \tfrac{\varepsilon_1}{q_{\perp,1}}(A_1 - B_1) &= \tfrac{\varepsilon_c}{q_{\perp,c}}(A_c e^{-iq_{\perp,c}\frac{L_c}{2}} - B_c e^{iq_{\perp,c}\frac{L_c}{2}}) \\ &+ \tfrac{\varepsilon_c}{q_{\perp,c}} \tfrac{4\pi i\omega}{c^2} \textstyle\sum_{\nu'=x,z} \sum_{\nu''=x,z} \int_{-\Lambda/2}^{\Lambda/2} dz' \int_{-\Lambda/2}^{\Lambda/2} dz'' G_{x,\nu'}\left(\omega, \vec{q}_{||}; -\tfrac{L_c}{2}, z'\right) \\ &\times \sigma_{\nu',\nu''}(\omega, \vec{q}_{||}; z', z'') E_{\nu''}(\omega, \vec{q}_{||}; z'') \end{aligned} \tag{3.54}$$

$$\begin{aligned} A_3 + B_3 &= A_c e^{iq_{\perp,c}\frac{L_c}{2}} + B_c e^{-iq_{\perp,c}\frac{L_c}{2}} \\ &- \tfrac{4\pi i\omega}{c^2} \textstyle\sum_{\nu'=x,z} \sum_{\nu''=x,z} \int_{-\Lambda/2}^{\Lambda/2} dz' \int_{-\Lambda/2}^{\Lambda/2} dz'' G_{x,\nu'}\left(\omega, \vec{q}_{||}; \tfrac{L_c}{2}, z'\right) \\ &\times \sigma_{\nu',\nu''}(\omega, \vec{q}_{||}; z', z'') E_{\nu''}(\omega, \vec{q}_{||}; z'') \end{aligned} \tag{3.55}$$

$$\begin{aligned} \tfrac{\varepsilon_1}{q_{\perp,1}}(A_3 - B_3) &= \tfrac{\varepsilon_c}{q_{\perp,c}}(A_c e^{iq_{\perp,c}\frac{L_c}{2}} - B_c e^{-iq_{\perp,c}\frac{L_c}{2}}) \\ &- \tfrac{\varepsilon_c}{q_{\perp,c}} \tfrac{4\pi i\omega}{c^2} \textstyle\sum_{\nu'=x,z} \sum_{\nu''=x,z} \int_{-\Lambda/2}^{\Lambda/2} dz' \int_{-\Lambda/2}^{\Lambda/2} dz'' G_{x,\nu'}\left(\omega, \vec{q}_{||}; \tfrac{L_c}{2}, z'\right) \\ &\times \sigma_{\nu',\nu''}(\omega, \vec{q}_{||}; z', z'') E_{\nu''}(\omega, \vec{q}_{||}; z'') \end{aligned} \tag{3.56}$$

for fixed ω an $\vec{q}_{||}$, since A_0 is the input while B_4 is usually taken to be zero, we have totally eight independent constants $B_0, A_1, B_1, A_c, B_c, A_3, B_3, A_4$ and a two-component electric

field function $E_x(\omega, \vec{q}_{||}, z)$, $E_z(\omega, \vec{q}_{||}, z)$ as unknown variables (functions), in which E_x and E_z are defined only in the SMC (including the QW). We stress that they are mutually coupled among each other through Eqs. (3.44), (3.46),(3.53)-(3.56) and the integral equation Eq.(3.49) (referring also to Eqs. (3.50) and (3.71)-(3.73). Since both Eqs. (3.44) and (3.46) are 2×2 matrix equations, the above listed equations are exactly mutually coupled eight algebraic equations and a two components integral equations which solve self-consistently the whole DBR–SMC(QW)–DBR system as long as we have the detailed expression for the conductivity tensor. Such a description [28] constitutes ourmathematical framework for studying the excitonic polaritons in the QW embedded in a SMC semiclassically. The pair of DBR's is coherently correlated with the SMC. It plays a role of modeselection. Therefore, the existing modes in the SMC not only dynamically couple to the semiconductor-medium in the QW, but also coherently coupled to the DBR's. That is the physical understanding for such a description.

Up to now, we finished the description for the medium polarization induced by the Coulomb interacting virtual electron-hole pairs in an intrinsic semiconductor QW at zero temperature. We notice that thez, z' dependence for the conductivity tensor Eq.(3.36) is separated in a bi-product of two ϕ-functions. By utilizing this property,following [28] , we can easily transform the integral equation (3.49) for the electric field in SMC into an algebraic equation which could further simplify the calculations. In particular, as $P^{(n;n',j_h)}_{n_{ex},l}(\omega, q_{||})$ has a resonant pole, only very a few even one discrete components for the electric field are needed. Introduce

$$\vec{F}^{(n;n',j_h)}_{n_{ex},l;l_h}(\omega, \vec{q}_{||}) = \int_{-\Lambda/2}^{\Lambda/2} dz \phi^{*(n;n',j_h)}_{n_{ex},l;l_h}(z) \vec{E}(\omega, \vec{q}_{||}; z) \tag{3.57}$$

meanwhile we may express the electric field in terms of $\vec{E}^{(n;n',j_h)}_{n_{ex},l;l_h}(\omega, \vec{q}_{||})$ as

$$\begin{aligned} \vec{E}(\omega, \vec{q}_{||}, z) = & \quad \vec{E}^{(c)}(\omega, \vec{q}_{||}, z) + \\ & \frac{4\pi e^2 p^2}{m^2 c^2} \sum_{n,n',j_h} \sum_{n_{ex},l,l_h} \int_{-\Lambda/2}^{\Lambda/2} dz' P^{(n;n',j_h)}_{n_{ex},l}(\omega, \vec{q}_{||}) G(\omega, \vec{q}_{||}, z, z') \\ & \phi^{(n;n',j_h)}_{n_{ex},l;l_h}(z) \cdot \eta^{(j_h,l,l_h)} \cdot \vec{F}^{(n;n',j_h)}_{n_{ex},l;l_h}(\omega, \vec{q}_{||}) \end{aligned} \tag{3.58}$$

with

$$\eta^{(j_h,l,l_h)} = \delta_{\mu\nu} \eta^{(j_h,l,l_h)}_{\mu} \tag{3.59}$$

We emphasize that $\vec{F}$-functions introduced by Eq.(3.57) depends on the electric field defined only in the region of $[-\frac{\Lambda}{2}, \frac{\Lambda}{2}]$, but the correspondent electric field has the expression as Eq.(3.58) is meaningful for the whole region of $[-\frac{L_c}{2}, \frac{L_c}{2}]$. Utilizing the above two equations,

we can express Eq.(3.49) as well as the boundary condition Eqs. (3.53)-(3.56) in terms of $\vec{F}$-functions following which our detailed calculations are proceeded.

The practical calculation is actually proceeded in such discrete form. Besides eq (3.57), we introduce further

$$\vec{f}^{(n;n',j_h)}_{n_{ex},l;l_h}(\omega,\vec{q}_{\|}) = \int_{-\Lambda/2}^{\Lambda/2} dz \phi^{*(n;n',j_h)}_{n_{ex},l;l_h}(z)\vec{E}^{(c)}(\omega,\vec{q}_{\|};z) \tag{3.60}$$

$$G^{(n;n',j_h;\ n'';n''',j'_h)}_{n_{ex},l,l_h;\ n'_{ex},l'l'_h}(\omega,\vec{q}_{\|}) = \int_{-\Lambda/2}^{\Lambda/2} dz \int_{-\Lambda/2}^{\Lambda/2} dz' \phi^{*(n;n',j_h)}_{n_{ex},l,l_h}(z) G(\omega;\vec{q}_{\|};z,z') \phi^{(n'';n''',j'_h)}_{n'_{ex},l',l'_h}(z') \tag{3.61}$$

then take the operation $\int_{-\Lambda/2}^{\Lambda/2} d.z\phi^{*(n;n',j_h)}_{n_{ex},l;l_h}(z)$ to both sides of Eq. (3.49), we obtain

$$\vec{F}^{(n;n',j_h)}_{n_{ex},l;l_h}(\omega,\vec{q}_{\|}) = \vec{F}^{(n;n',j_h)}_{n_{ex},l;l_h}(\omega,\vec{q}_{\|}) + \frac{4\pi e^2 p^2}{m^2c^2} \times \sum_{n'',n''',j'_h} \sum_{n'_{ex},l',l'_h} G^{(n;n',j_h;\ n'';n''',j'_h)}_{n_{ex},l,l_h;\ n'_{ex},l'l'_h}(\omega,\vec{q}_{\|}) P^{(n'';n''',j'_h)}_{n'_{ex},l'}(\omega,\vec{q}_{\|}) \cdot \cdot \eta^{(j'_h,l',l'_h)} \cdot \vec{F}^{(n'';n''',j'_h)}_{n'_{ex},l';l'_h}(\omega,\vec{q}_{\|}) \tag{3.62}$$

The boundary condition Eqs. (3.56) can also be reformulated in terms of $F^{(n;n',j_h)}_{n_{ex},l;l_h}$ as

$$A_1 + B_1 = A_c e^{iq_{\perp,c}L_c/2} + B_c e^{iq_{\perp,c}L_c/2} + \frac{4\pi e^2 p^2}{m^2c^2} \sum_{n,n',j_h} \sum_{n_{ex},l,l_h} \sum_{\mu} \int_{-\Lambda/2}^{\Lambda/2} dz' P^{(n;n',j_h)}_{n_{ex},l}(\omega,\vec{q}_{\|}) G_{x,\mu}\Big(\omega,\vec{q}_{\|};-\frac{L_c}{2},z'\Big) \times \phi^{(n;n',j_h)}_{n_{ex},l;l_h}(z') \eta^{(j_h,l,l_h)}_{\mu} F^{(n;n',j_h)}_{n_{ex},l;l_h;\mu}(\omega,\vec{q}_{\|}) \tag{3.63}$$

$$\frac{\varepsilon_1}{q_{\perp,1}}(A_1 - B_1) = \frac{\varepsilon_c}{q_{\perp,c}}(A_c e^{-iq_{\perp,c}L_c/2} - B_c e^{iq_{\perp,c}L_c/2}) - \frac{\varepsilon_c}{q_{\perp,c}} \frac{4\pi e^2 p^2}{m^2c^2} \sum_{n;n',j_h} \sum_{n_{ex},l,l_h} \sum_{\mu} \int_{-\Lambda/2}^{\Lambda/2} dz' P^{(n;n',j_h)}_{n_{ex},l}(\omega,\vec{q}_{\|}) \times G_{x,\mu}\Big(\omega,\vec{q}_{\|};-\frac{L_c}{2},z'\Big) \phi^{(n;n',j_h)}_{n_{ex},l;l_h}(z') \eta^{(j_h,l,l_h)}_{\mu} F^{(n;n',j_h)}_{n_{ex},l;l_h;\mu}(\omega,\vec{q}_{\|}) \tag{3.64}$$

$$A_3 + B_3 = A_c e^{iq_{\perp,c}L_c/2} + B_c e^{-iq_{\perp,c}L_c/2} \frac{4\pi e^2 p^2}{m^2c^2} \sum_{n,n',j_h} \sum_{n_{ex},l;l_h} \sum_{\mu} \int_{-\Lambda/2}^{\Lambda/2} dz P^{(n;n',j_h)}_{n_{ex},l}(\omega,\vec{q}_{\|}) G_{x,\mu}\Big(\omega,\vec{q}_{\|};\frac{L_c}{2},z'\Big) \times \phi^{(n;n',j_h)}_{n_{ex},l;l_h}(z') \eta^{(j_h,l,l_h)}_{\mu} F^{(n;n',j_h)}_{n_{ex},l;l_h;\mu}(\omega,\vec{q}_{\|}) \tag{3.65}$$

$$\frac{\varepsilon_1}{q_{\perp,1}}(A_3 - B_3) = \frac{\varepsilon_c}{q_{\perp,c}}(A_c e^{iq_{\perp,c}L_c/2} + B_c e^{-iq_{\perp,c}L_c/2}) + \frac{\varepsilon_c}{q_{\perp,c}} \frac{4\pi e^2 p^2}{m^2c^2} \sum_{n;n',j_h} \sum_{n_{ex},l,l_h} \sum_{\mu} \int_{-\Lambda/2}^{\Lambda/2} dz' P^{(n;n',j_h)}_{n_{ex},l}(\omega,\vec{q}_{\|}) \times G_{x,\mu}\Big(\omega,\vec{q}_{\|};\frac{L_c}{2},z'\Big) \phi^{(n;n',j_h)}_{n_{ex},l;l_h}(z') \eta^{(j_h,l,l_h)}_{\mu} F^{(n;n',j_h)}_{n_{ex},l;l_h;\mu}(\omega,\vec{q}_{\|}) \tag{3.66}$$

Then, in terms of the discrete representation for the electric field $\vec{F}^{(n;n',j_h)}_{n_{ex},l;l_h}(\omega,\vec{q}_{\|})$, the complete description for the DBR-SMC(QW)-DBR system now is by the Eqs. (3.44),(3.46),(3.64)-(??) and (3.62) referring also to Eqs. (3.50),(3.73),(3.57), (3.58)and (3.60). Up to now, it is enough clear that we do not need the effective photon-exciton coupling constant anymore in the approach we engaged.

3.4 Results and discussions

We discuss a pair of symmetric DBR's. One of the two alternating layers usually is taken as $Al_{0.15}Ga_{0.85}As$ with its dielectric constant $\varepsilon_1 = 13$ and thickness L_1, the other layer is chosen as AlAs with a dielectric constant $\varepsilon_2 = 9.49$ and of the thickness L_2. The cavity material is as $Al_{0.3}Ga_{0.7}As$ which has a dielectric constant as ε_c= 12.04. We take the QW material as GaAs which is approximately of the same dielectric constant as ε_c. In this paper, we assume the thickness of the QW $\Lambda = 100$Å. The energy gap E_g for the QW is of 1.428 ev. We solve $\varphi^{(c)}_n(z)$ and $\varphi^{(v)}_{n',j_h;\alpha'}(k_{\|}z)$ of Eqs. (2.16) and (2.17) from Hamiltonian Eqs. (2.10) and (2.11) infinitely highbarrier approximation. The former can be solved analytically with conduction electron mass $m^{(c)}_{\perp}$ taken as 0.067 m_e. We may derive the correspondent value of ϵ^c_n as $\frac{\hbar^2}{2m^{(c)}_{\perp}}(\frac{\pi}{\Lambda})^2n^2$ with $n = 1, 2, \cdots$. The latter has to be solved numerically[32]. We then derive the $\epsilon^{(v)}_{n',j_h}$ as the value of numerical function $\epsilon^{(v)}_{n',j_h}(k_{\|})$ at $k_{\|} = 0$, derive further the effective mass $m^{(v)}_{n',j_h;\|}$ from the curvature of $\epsilon^{(v)}_{n',j_h}(k_{\|})$ at $k_{\|} = 0$. Utilizing $m^{(c)}_{\|}$= 0.067 m_e and $m^{(v)}_{n',j_h;\|}$ we can introduce the 2D center of mass coordinate as well as the reduced mass, and further derive the $\epsilon^{(n;n',j_h)}_{\vec{q}_{\|}}$, $\epsilon^{(n;n',j_h)}_{n_{ex},l}$ and $f^{(n;n',j_h)}_{n_{ex},l}(k_{\|})$ by the known solution of 2D hydrogen atom approximation bur the effective Bohr radius take the variation results of the reference[25]. All the above results constitute the necessary ingredients to calculate $\phi^{(n;n',j_h)}_{n_{ex},l;l_h}(z)$ and $P^{(n;n',j_h)}_{n_{ex},l}(\omega,\vec{q}_{\|})$ up to a set of phenomenological parameters as the width for the excitonic levels. Here we choose all these γ's equal to 0.05 mev for a preliminary study. We can then solve self-consistently the set of coupled equations (3.44), (3.46) (3.63)-(3.66) and (3.62) for the symmetric DBR-SMC(QW)-DBR system. We notice that, in the detailed calculations, various kinds of energies are scaled by $\frac{\hbar^2}{2m}(\frac{\pi}{\Lambda})^2$= 3.76 mev, all the wave vector are scaled by $\frac{\pi}{L_c}$ and the amplitude for the electric fields are scaled by A_0.

Eq.(3.58) in conjunction with expressions (3.37) and (3.57) shows explicitly how the non-locality for the conductivity behaves. Each term of the spectral weight function has a form of a product of two ϕ-functions with one of the two depending only on z while other depending

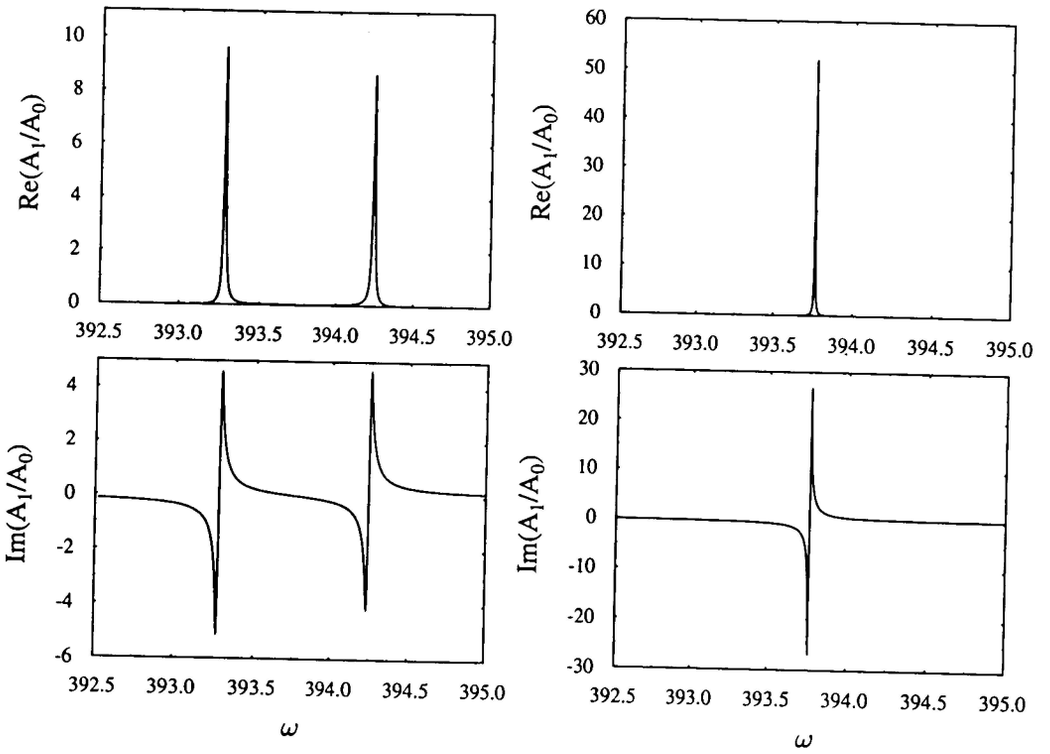

Figure 3.3: Electric field components A_1 versus frequency ω for the SMC arround the 1CB-1HH 1s exciton-polariton resonance (left), and compared with that for the empty SMC (right).

on z' separately, therefore, one of which is convoluted with the electric field played a role as its "weight" function and the other is convoluted with the Green's function as its "source" function, which strongly influences the effective coupling between light and the exciton.

We tune the frequency of the incident light very close to the HH exciton state with $n_{ex} = 1$, $l = 0$, $n = n' = 1$, $j_h = \frac{3}{2}$ and consider the case of normal incidence with $\vartheta = 0$. Meanwhile each DBR with 30 paired layers isassumed satisfying the $\frac{\lambda}{4}$ condition for each layer, the length of the SMC is equal to the half wave length as $L_c = \frac{\lambda}{2}$. As a reference system, we first repeat the known results for the DBR-SMC-DBR system without the QW but with our parameters. We have only almost one electromagnetic mode propagating through the system which has a frequency located at the center for 30- double layered DBR's forbidden band as $\omega_0 = 393.8$. It has a narrow width only of γ_0=0.0203mev. The correspondent electric

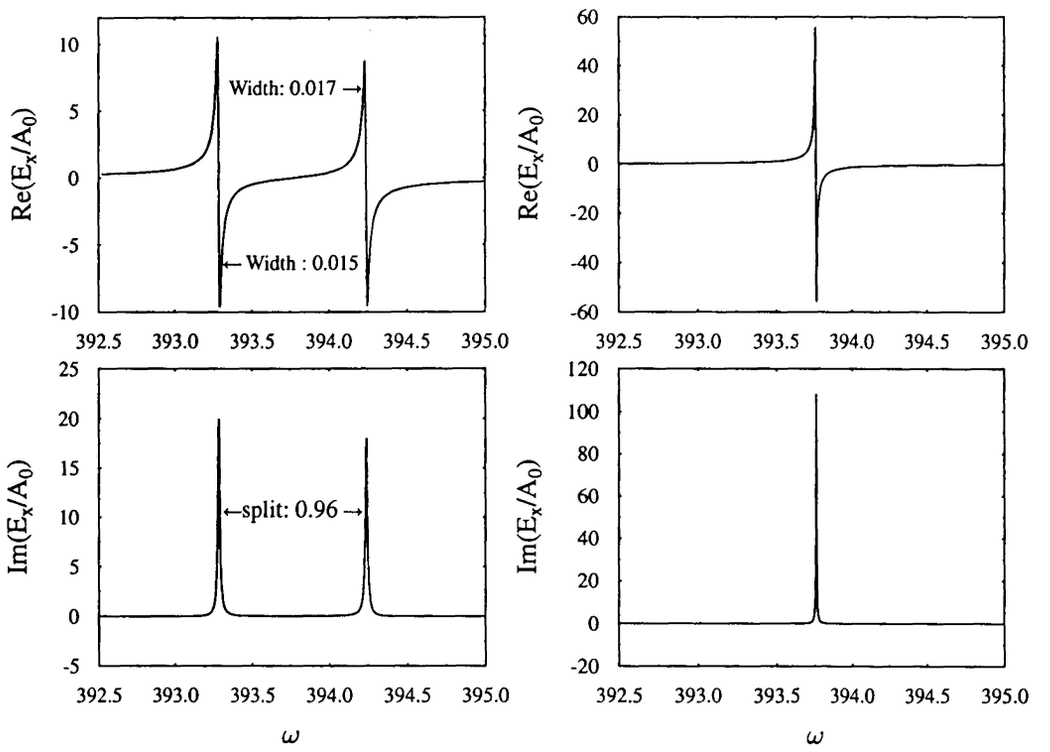

Figure 3.4: The Electric field at the center ($z = 0$) $A_c + B_c$ versus frequency ω for the SMC near the 1CB-1HH 1s exciton-polariton resonance (left), and compared with that for the empty SMC (right).

field amplitudes (versus frequency) at various typical points of the system as A_1, A_c+B_c, A_4, B_0 are shown in the right parts of Fig. 3.3, 3.4, 3.5 for the whole DBR-SMC-DBR system. In particular, all the frequency dependence of the real parts of these amplitudes matches that of their imaginary parts in a Lorentzian way.

We then sandwich the QW into the SMC. It appears two slitted sharp peaks in the observable $1 - |r|^2 - |t|^2$, kwown as the Rabi splitting, shown in the Fig. 3.7, where $r = B_0$ is the reflection coefficient and $t = A_4$ is the transmission coefficient.. The calculated split between the two peaks is $\sim$ 3.6 mev, while the simple dielectrc model gives $\sim$ 3.2mev for which oscillator strength is taken as $\sim 3 \times 10^{12} cm^{-1}$[26][33]. The calculation shows that there are two correspondent peaks not only in the spectrum for the electric field amplitude at the

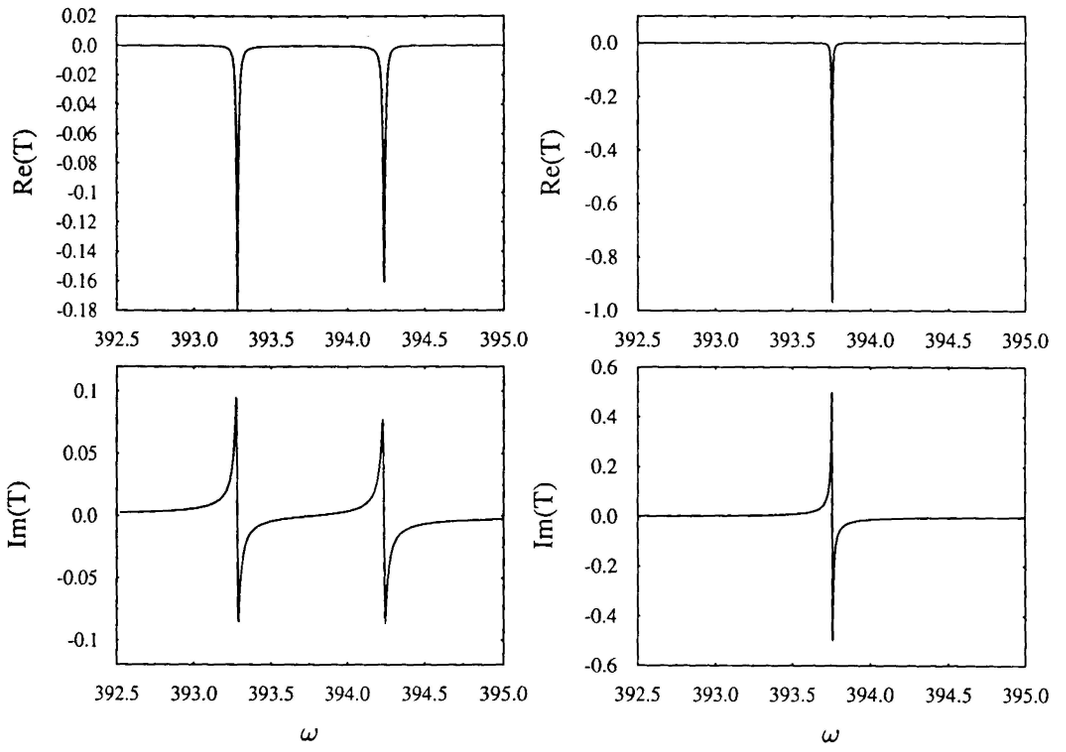

Figure 3.5: Electric field components A_4 (transmission) versus frequency ω for the SMC arround the 1CB-1HH 1s exciton-polariton resonance (left), and compared with that for the empty SMC (right).

center of the QW as shown in the right part of Fig. 3.4, but also in A_1, A_4 andB_0 as shown in the right parts of Fig. 3.3, 3.5 and 3.6 respectively. We understand there are two branches of excitonic polaritons formed in the QW, but extend throughout the DSR-SMC(QW)-DBR system with the phase coherence being precisely kept. It is resonableto interpret them as the two "unified" physical modes for the whole system. We may label these polaritons in terms of the hybridizing excitonic quantum numbers. one of the distinguished feature for this approach, it makes the important role of the parity symmetry along z-axis to be explicit. It can also be viewd as then consequence of the non-locality. Here we restrict ourself for the case of normal incidence andsymmetric DBR pairs only. As we have discussed in Sec. II-B, the $\varphi_n^{(c)}(z)$ and $\varphi_{n,j_h;\alpha'}^{(v)}(k_{\|}z)$ can be classified by the parity symmetry (along z-axis).In

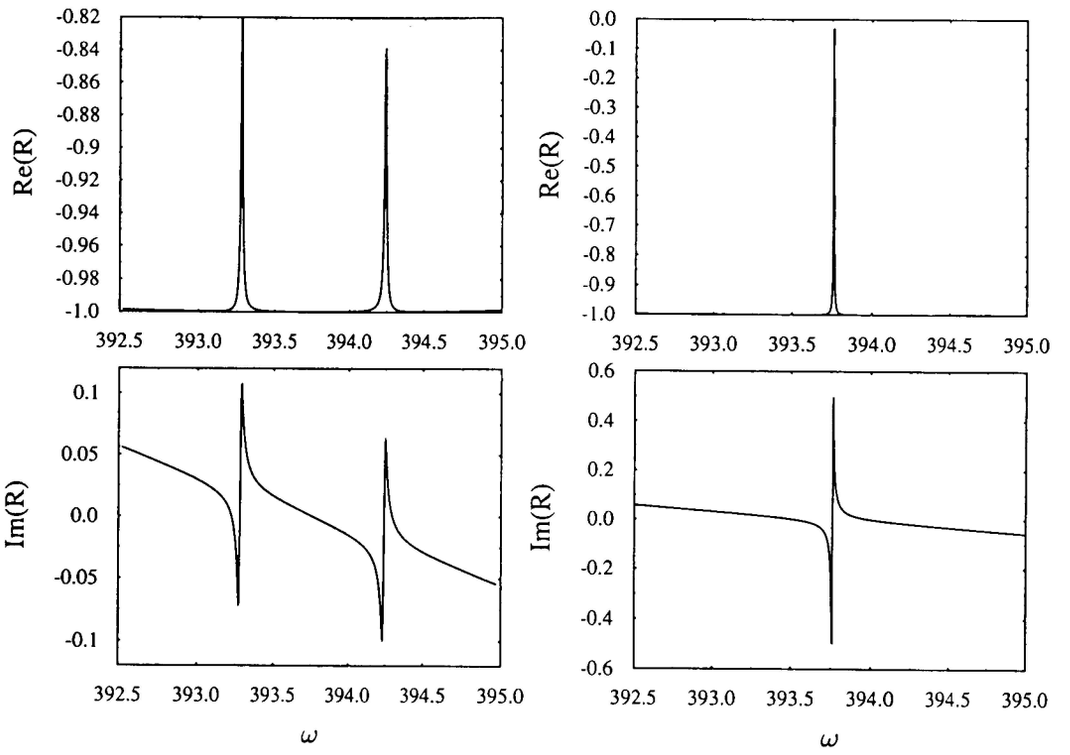

Figure 3.6: Electric field components B_0 (reflection) versus frequency ω for the SMC arround the 1CB-1HH 1s exciton-polariton resonance (left), and compared with that for the empty SMC (right).

fact, the parity symmetry for the contributed component ofthe hole spinor wave functions is controlled by its index $\alpha' = j_h + l_h$. Moreover, for a SMC confined by a pair of symmetric DBR's, it is known that $\vec{E}^{(c)}(\omega, \vec{q}_{||}; z)$ as a functionof z is also an eigenstates of the parity symmetry at the resonant condition $L_c = \frac{n}{2}\lambda$ with $n = 1, 2, \cdots$ (see Fig. 3.8). By considering Eqs. (3.49), (3.73), (3.36) and (3.37), we can verify that the electric field $\vec{E}(\omega, \vec{q}_{||}; z)$ will have the same even-oddness as that of $\vec{E}^{(c)}(\omega, \vec{q}_{||}; z)$.

Now following Eq.'s (3.58), (3.43) and (3.37), the physics contributed by the QW depends strongly on the integral

$$I_{l_h}^{(n;n',j_h)}(\omega, \vec{q}_{||}; k_{||}) = \int_{-\Lambda/2}^{\Lambda/2} dz \varphi_n^{(c)}(z) \varphi_{n',j_h;\alpha'=j_h+l_h}^{(v)}(k) E_x(\omega, \vec{q}_{||}; z), \tag{3.67}$$

we can then find its interesting consequence for the polaritons. If we set the $\varphi_n^{(c)}(z)$ for the

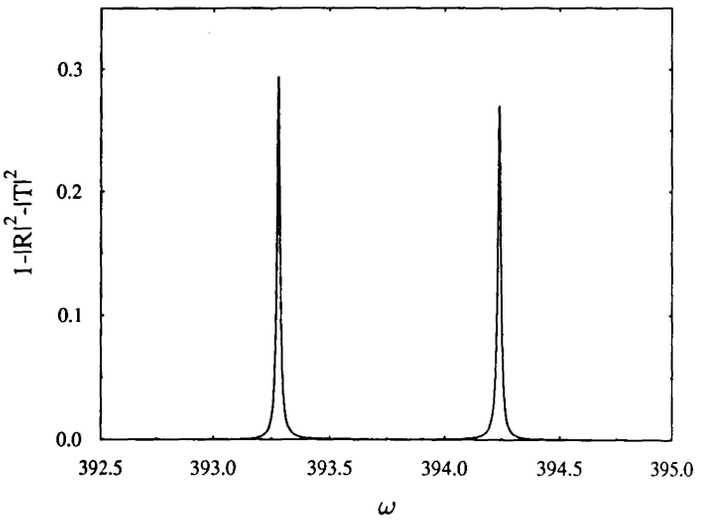

Figure 3.7: The absorption versus frequency ω for the SMC around the 1CB-1HH 1s exciton-polariton resonance.

conduction electron always stay in the $n = 1$ state, it will not contribute to the paritysymmetry discussion undergoing since it is an even function of z. As shown in Fig. 3.8, the $E^{(c)}(\omega, q_{\|}; z)$ is even for$L_c = \frac{\Lambda}{2}$ while odd for $L_c = \lambda$. So for a SMC of $L_c = \frac{\Lambda}{2}$, the electric field is even. Then, following Eq.(3.31), only polaritons with quantum number$l = l_h = 0$ and the index $\alpha' = j_h$ can survive in the SMC for both$j_h = \frac{1}{2}$ and $j_h = \frac{3}{2}$. This because$\varphi^{(v)}_{n'=1,j_h;\alpha'=j_h}(k_{\|}z)$ is an evenfunction of z. Those hybridization induced polaritons with quantum number $l = 1$ cannot be observed since $\varphi^{(v)}_{n'=1,j_h;\alpha'=j_h\pm1}(k_{\|}z)$ are oddfunctions of z which will make$I^{(1;1,j_h)}_{l_h=\pm1(\omega,\vec{q}_{\|};k_{\|})} = 0$. On the contrary, if we have a SMC of $L_c = \lambda$, the electric field $E_x(\omega, \vec{q}_{\|}; z)$ becomes an odd function of z, meanwhile $\varphi^{(v)}_{n'=1,j_h;\alpha'=j_h}(k_{\|}z)$ isstill an even function, the polaritons with quantum number $n = n' = 1$, $l = 0$ will be forbidden for the λ-SMC which will make $I^{(1;1,j_h)}_{l_h}(\omega, \vec{q}_{\|}; k_{\|}) = 0$. In this case, only the hybridization induced polariton can survive in the SMC since $\varphi^{(v)}_{n'=1,j_h;\alpha'=j_h\pm l_h}(k_{\|}z)$ is odd. Generally, the parity of $\varphi^{(c)}_n(z)$ and $\varphi^{(v)}_{n',j_h;\alpha'=j_h}(k_{\|}z)$ is the same. If $L_c = \frac{m+1}{2}\lambda$, the selection rule can be summarized into:

$$n - n' + l_h + m = even \tag{3.68}$$

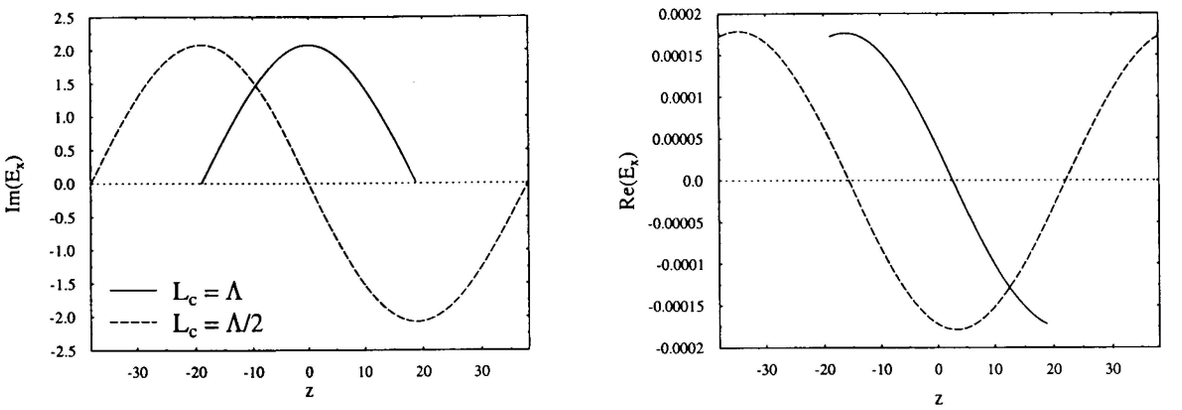

Figure 3.8: The electric field distribution along z axis for the empty SMC (without QW embedded) at the resonant frequency.

It is necessary to compare the QW-embedded SMC case with isolated QWs. In the latter, the exciton light transition element is only proportional to:

$$T_{l_h}^{(n;n',j_h)}(\omega;k_{\|}) = \int_{-\Lambda/2}^{\Lambda/2} dz\varphi_n^{(c)}(z)\varphi_{n',j_h;\alpha'=j_h+l_h}^{(v)}(k_{\|}z) \tag{3.69}$$

Like the above arguement, the selection rule is:

$$n - n' + l_h = even \tag{3.70}$$

What we learned from the above discussion is that the even-oddness for the electric field depends on the cavity resonance condition while the parity of the components for the electron or hole wave function depends only on the QW. Then we can have an interplay of the even-odd symmetry for the integrand of Eq.(3.57). As a result the parity symmetry along z-axis will provide a sort of selection rule for the forbidden polaritons in a symmetric DBR pair confined resonant SMC. It could be rather helpful for searching the hybridization induced polaritons.

As an example for the hybridization induced polaritons, in this paper, for reason of comparison, we would like to explore in detail the HH subband dominated polaritons which has the quantum numbers as n=1, n'=2, j_h=$\frac{3}{2}$, $n_{ex} = 2$, $l = 1$. We have to tune the frequency for the incident light higher to match the correspondent energy level. As shown in Fig. 3.11

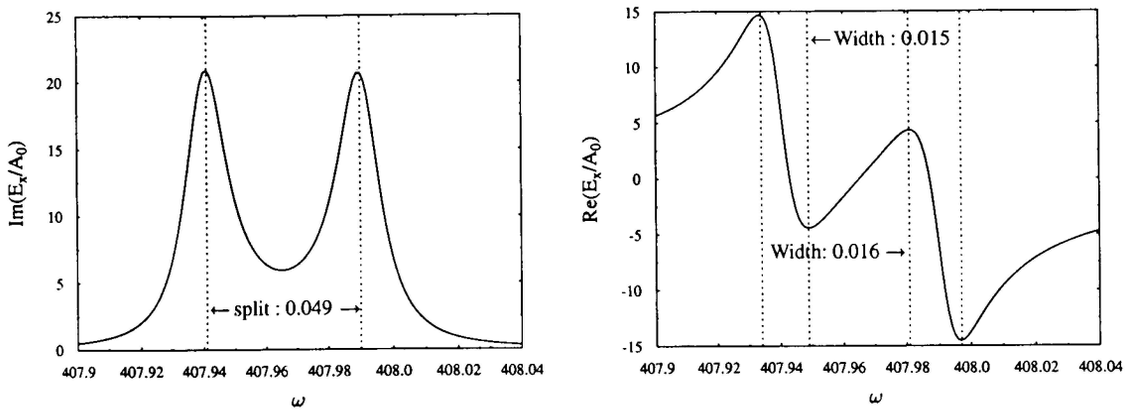

Figure 3.9: Electric field at the center($z = 0$) versus frequency for the SMC around the 1CB-2HH 2p exciton-polariton resonance.

and 3.9, our calculation does find two Rabi splitting modes. The splitting has a value as 0.066 ($\sim$ 0.2 mev). These two modes still have a Lorentzian form respectively with a width of $\sim$ 0.016 for each of them. In particular, the incident angle dependence for the magnitude of the first peak in $1 - |r|^2 - |t|^2$ has a quite different behavior from that of the $n = n' = 1$, $j_h = \frac{3}{2}$, $l = 0$ polariton which is shown in Fig 3.10. We notice that such difference is partially due to the difference of $(\eta_x^{(3/2,0,0)}, \eta_z^{(3/2,0,0)}) = (1, 0)$ while $(\eta_x^{(3/2,1,-1)}, \eta_z^{(3/2,1,-1)}) = (\frac{1}{3}, \frac{4}{3})$. We wish it could be also helpful for the experimental observation for such hybridization induced polaritons.

As a further application of our approach, we studied also the incident angle dependence of the absorption of the p-polaruized light for the LH induced excitonic polaritons in the SMC of $L_c = \frac{\lambda}{2}$ with our notation as $n = n' = 1$, $j_h = \frac{1}{2}$, $n_{ex} = 1$, $l = 0$. In the strong coupling region, as expected for the normal incidence, we have the Rabi splitting smaller than that of the HH induced ($j_h = \frac{3}{2}$), mainly due to that $\eta_x^{(1/2,0,0)}$ is only one third of $\eta_x^{(3/2,0,0)}$ as we can see in Fig. 3.12. When the incident angle ϑ increases from zero, the lower frequency peak moves accordingly towards the corespondent excitonic level while the higher frequency peak increases its frequency very fast. Both peakes die down versus increasing incident angle gradually. What rather interested us is that, beyond certain value of the incident angle which is around $15° \sim 20°$, a new weakly splitted peaks close to the exciton

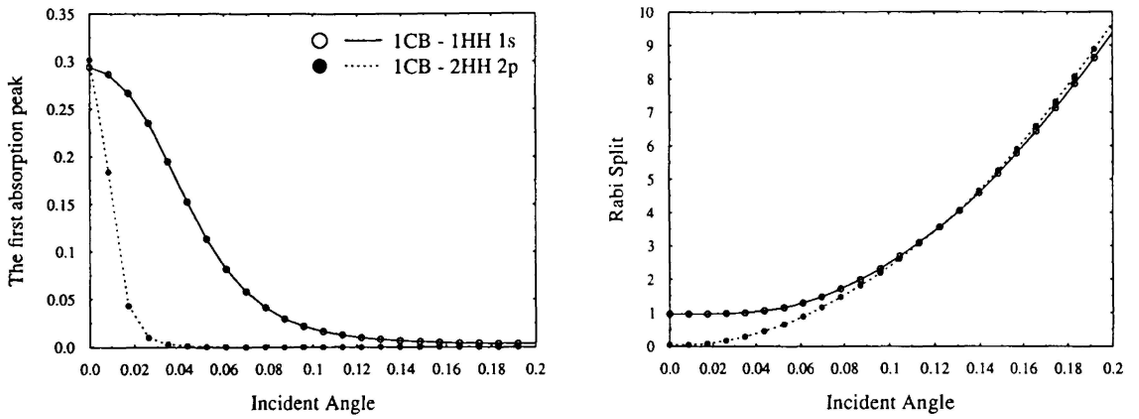

Figure 3.10: The anglar dependences of the amplitude of the first absorption peak and Rabi splitting for the 1CB-1HH 1s exciton-polariton resonace compared with that for 1CB-2HH 2p exciton-polariton

level occurs . It grows up gradually with the further increasing of ϑ. We understand that it means that the perpendicular component of the electric field starts to exhibite its nontrivial role in the coupling with the LH exciton. Such weak splitting is absent for the corresponding HH exciton case as its $\eta_z^{(3/2,0,0)} = 0$. It is actuallty a results of the coupling of LH exciton and TM like photon mode of the system. Althrough the splittingis so small and the incident angle is a bit large, this interesting phenomena could be rather difficult to be obsevated, we still hope that our finding will stimulate further study and be tested experimentally. Meanwhile it shows one of advantage of our approach.

In conclusion, we presented a self-consistent semiclassical approach for exciton-polariton in QW embedded in SMC. In this approach, the effect of the complex valence band structure and the non-locality of the dielectric response of the exciton in QW are carefully accounted. We show that 2P exciton can also couple with photon mode and forms polariton. For symmetric SMC, our analysis gives a "selection rule" in forming exciton-polaritons, which is essentially an interplay among the angular quantum numbers of excitons, the electron-hole subbands indices and the resonance conditions of the SMC. We also show that, for LH exciton-polariton, due to the coupling with the axial component of the p-polarized light wave, it will appear one another splitted peaks when the incident angle exceeds certain

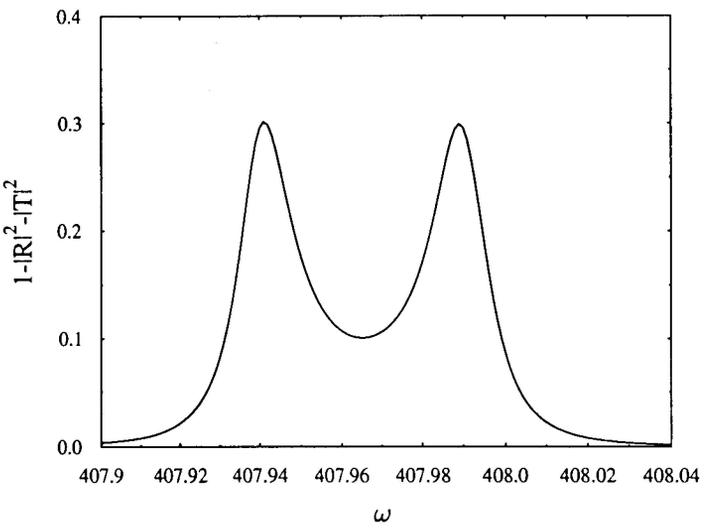

Figure 3.11: Absorption versus frequency ω for the SMC arround the 1CB-2HH 2p exciton-polariton resonance.

range.

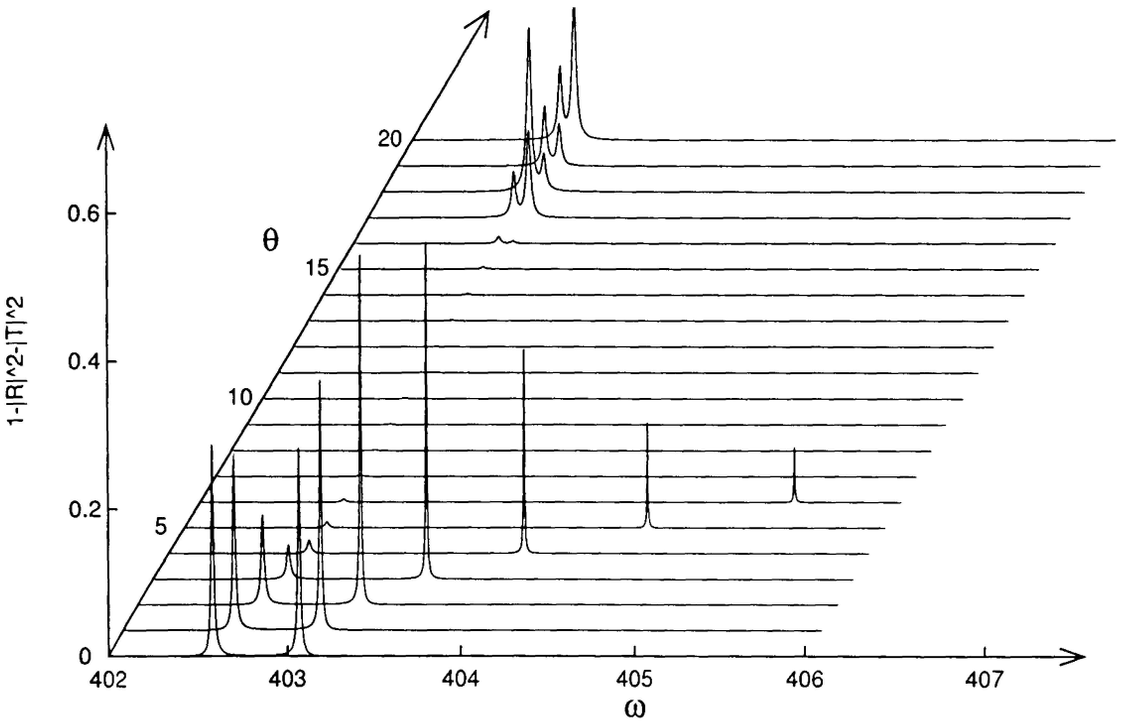

Figure 3.12: The absorption of the SMC versus frequncy ω and the incident angle θ(degree) around the 1CB-1LH 1s exciton-polariton resonance.

Appendix: The Expressions for the Transfer Matrix Elements and the Green's Functions

The transfer matrix elements can be calculated straightforwardly as[29]

$$\begin{aligned} t_{11}^{L} &= e^{-iq_{\perp,1}L_1}\Big[\cos(q_{\perp,2}L_2) - \tfrac{i}{2}\Big(\tfrac{\varepsilon_2 q_{\perp,1}}{\varepsilon_1 q_{\perp,2}} + \tfrac{\varepsilon_1 q_{\perp,2}}{\varepsilon_2 q_{\perp,1}}\Big)\sin(q_{\perp,2}L_2)\Big] \\ t_{12}^{L} &= e^{iq_{\perp,1}L_1}\Big[-\tfrac{i}{2}\Big(\tfrac{\varepsilon_2 q_{\perp,1}}{\varepsilon_1 q_{\perp,2}} - \tfrac{\varepsilon_1 q_{\perp,2}}{\varepsilon_2 q_{\perp,1}}\Big)\sin(q_{\perp,2}L_2)\Big] \\ t_{21}^{L} &= e^{-iq_{\perp,1}L_1}\Big[\tfrac{i}{2}\Big(\tfrac{\varepsilon_2 q_{\perp,1}}{\varepsilon_1 q_{\perp,2}} - \tfrac{\varepsilon_1 q_{\perp,2}}{\varepsilon_2 q_{\perp,1}}\Big)\sin(q_{\perp,2}L_2)\Big] \\ t_{22}^{L} &= e^{iq_{\perp,1}L_1}\Big[\cos q_{\perp,2}L_2 - \tfrac{i}{2}\Big(\tfrac{\varepsilon_2 q_{\perp,1}}{\varepsilon_1 q_{\perp,2}} + \tfrac{\varepsilon_1 q_{\perp,2}}{\varepsilon_2 q_{\perp,1}}\Big)\sin(q_{\perp,2}L_2)\Big] \end{aligned} \tag{3.71}$$

and

$$\begin{aligned} t_{11}^{R} &= t_{11}^{L}\,, & t_{22}^{R} &= t_{22}^{L}, \\ t_{12}^{R} &= -t_{21}^{L}\,, & t_{21}^{R} &= -t_{12}^{L}, \end{aligned} \tag{3.72}$$

Moreover, the Green's functions in Eq. (3.51) can also be easilysolved as[30]

$$\begin{aligned} G_{x,x}(\omega, q_{\|}; z, z') &= -\tfrac{ic^2}{2\omega^2\varepsilon_c(\omega)} q_{\perp,c} e^{iq_{\perp,c}|z-z'|} \\ G_{x,z}(\omega, q_{\|}; z, z') = G_{z,x}(\omega, q_{\|}; z, z') &= \tfrac{ic^2}{2\omega^2\varepsilon_c(\omega)} q_{\|} Sgn(z-z') e^{iq_{\perp,c}|z-z'|} \\ G_{z,z}(\omega, q_{\|}; z, z') &= \tfrac{c^2}{\omega^2\varepsilon_c(\omega)}\delta(z-z') - \tfrac{ic^2}{2\omega^2\varepsilon_c(\omega)} \tfrac{q_{\|}^2}{q_{\perp,c}} e^{iq_{\perp,c}|z-z'|} \end{aligned} \tag{3.73}$$

Chapter 4

Squeezing of excitonic polariton

M.Artoni and L.Birman first pointed out that excitonic polariton quantum states are squeezed state [35]. The double-photon term is indispensible to the origin of squeezing which is induced by canocial momentum. Namely, the interaction between electromagnetic field and exciton contributes to the squeezing. It follows naturally in SMC the effect can be enhanced. We can employ quantum optics in cavity into such problems. So in this chapter, our fashion of studying is quite different from last chapter. We have to neglect the valence band coupling and the comlex energy level of exciton. However, The diagonalization of Hamiltonian has its own advantages. The hybridization of photon and exciton is obvious in this representation; besides, the dispersion and squeezing relation can be given in an analytical form.

4.1 Interaction Hamiltonian between QW excitons and light in SMC

The interaction can be written in two parts:

$$H_{int}^{(1)} = \sum_{k,q} A_{k,q}(a_{k,q} + a_{-k,q}^{\dagger})(b_k^{\dagger} + b_{-k}) \tag{4.1}$$

$$H_{int}^{(2)} = \sum_{k,q,q'} \frac{A_{k,q}A_{k,q'}}{\hbar\omega_k}(a_{-k,q} + a_{k,q}^{\dagger})(a_{k,q'} + a_{-k,q'}^{\dagger}) \tag{4.2}$$

k is the wave vector in $X-Y$ plane and q, q' is wave vector along growth direction. $a_{k,q}$ and b_k is the annihilation operator of phton and exciton respectively. The coupling constant is

$$A_{k,q} = i\frac{2p\phi(0)}{m}\sqrt{\frac{\hbar}{\epsilon_b L_c}}\frac{1}{(k^2+q^2)^{1/4}}I(k,q) \tag{4.3}$$

in which m is electron mass, ϵ_b is background dielectric constant, $p = \langle X|p_x|s\rangle = \langle Y|p_y|s\rangle = \langle Z|p_z|s\rangle$ as mentioned in last chapter. $\phi(0)$ is the zero point value of relative motion wavefuction of exciton in real space. L_c is the length of cavity. $I(q)$ is the overlap between exciton envelop function and mode function of cavity $u_q(z)$:

$$I(k,q) = \int_{-L_c/2}^{L_c/2} dz\varphi^{(c)}(z)\varphi^{(v)}(k;z)u_q(z) \tag{4.4}$$

We have analysed the important consequence of this integral on the selection rule of optical spectrum.

During the derivation of the above Hamiltonian, several approximations have been used. We single out one exciton state (e.g.1CB-1HH) and only s state of relative motion is considered which dominates in light transition when coupling effect is neglectable. Finally, the dipole interaction approximation has been made.

It is still difficult to solve the Hamiltonian exactly even though we made the above assumptions. As mentioned before, only one eletromagnetic mode in the cavity plays an important role, since SMC is so tiny that the separation between various mode is very big. Usually it is greater than the working bandwidth of laser. So we can just keep the privileged mode in the interaction of light and exciton and leave other modes as a loss of cavity. With this consideration, we can simplify the Hamiltonian further:

$$H = \sum_{k\geq 0}(H_k + H_{-k}) + h.c. \tag{4.5}$$

in which

$$H_k = E_k^{ex}(b_k^\dagger b_k + 1/2) + E_k^{ph}(a_k^\dagger a_k + 1/2) + A_k(a_{-k}b_k + a_k^\dagger b_k) + B_k a_k a_{-k} + a_k^\dagger \Gamma_k^{ph} + b_k^\dagger \Gamma_k^{ex} \tag{4.6}$$

with half exciton energy $E_k^{ex} = \hbar\omega_k/2$ and half photon energy $E_k^{ph} = \hbar c|\vec{k} + \vec{q}^*|/2$ and the coupling constant is $A_k = A_{k,q_n}$. $q^* = \frac{\pi}{L_c}$ which corresponds to privileged mode. Γ_k^{ph} and Γ_k^{ex} are the total loss for photon and exciton including the contribution of un-privileged mode and other damping sources such as phonons. Double-photon term is

$$B_k = |A_k|^2/4E_k^{ex} \tag{4.7}$$

We note that exciton energy has two parts: the center of mass kinetic energy and relative motion energy:

$$\hbar\omega_k = \frac{\hbar^2 k^2}{2M_{ex}} + \varepsilon_{ex} \tag{4.8}$$

M_{ex} is exciton mass. We have the explicit form of ε_{ex} in last chapter.

4.2 Squeezing of polariton

We introduce polariton state operators

$$\begin{aligned} c_k &= \cos\theta_k a_k + i\sin\theta_k b_k \\ c_{-k} &= \cos\theta_{-k} a_{-k} + i\sin\theta_{-k} b_{-k} \end{aligned} \tag{4.9}$$

If the double-photon term is omitted, it is easy to diagonalize the Hamiltonian in a free particle form of c_k and c_{-k}. When the motion equation is solved, we can see clearly that the system is a hybridized wave changing from photon to exciton, then from exciton to photon, back and forth. The period of oscillation is called Rabi period.

However, B_k is the important factor that leads to squeezing. It is well known that we can introduce Bogoliubov transformation to diagonalize the full Hamiltonian (4.6) with the presence of quadratic term of creative operator or annihilation operator

$$\begin{aligned} \eta_k &= wa_k + xb_k + ya_{-k}^\dagger + zb_{-k}^\dagger \\ \eta_{-k} &= wa_{-k} + xb_{-k} + ya_k^\dagger + zb_k^\dagger \end{aligned} \tag{4.10}$$

We can put it into a more exlicit way in which the squeezing property is obvious

$$\begin{aligned} \eta_k &= Sc_kS^\dagger = c_k\cosh r + c_{-k}^\dagger e^{i2\varphi}\sinh r \\ \eta_{-k} &= Sc_{-k}S^\dagger = c_{-k}\cosh r + c_k^\dagger e^{i2\varphi}\sinh r \end{aligned} \tag{4.11}$$

Here

$$S = \exp\left[r(-c_k^\dagger c_{-k}^\dagger e^{2i\varphi} + c_k c_{-k} e^{-2i\varphi})\right] \tag{4.12}$$

is a two-mode squeeze operator. r is squeezing factor which measures the degree of squeezing of the quantum noise. φ is squeezing angle which is the relative phase difference between the maximum-squeezed quadrature and the regular quadrature in phase space.

After these procedures, one finds

$$H_k = E_k(\eta_k^\dagger\eta_k + 1/2) \tag{4.13}$$

with

$$E_k^2 = 2[(E_k^{ph})^2 + (E_k^{ex})^2 + \frac{A_k^2 E_k^{ph}}{E_k^{ex}}] \pm 2\sqrt{[(E_k^{ph})^2 - (E_k^{ex})^2]^2 + 2[(E_k^{ph})^2 + (E_k^{ex})^2]\frac{A_k^2 E_k^{ph}}{E_k^{ex}} + (\frac{A_k^2 E_k^{ph}}{E_k^{ex}})^2} \quad (4.14)$$

The upper branch and lower branch of energy constitute a complete dispersion relation of polariton. Temporarily we neglect the damping term which would not alter the main structure of the spectrum and only contributes a finite broadening.

The squeezing factor r can be proved to satisfy the following

$$\tanh r = \sqrt{\frac{R_1^2 + R_2^2}{R_3^2 + R_4^2}} \quad (4.15)$$

in which

$$\begin{aligned}
R_1 &= \frac{(E_k - 2E_k^{ph})(4(E_k^{ex})^2 - E_k^2)}{4E_k^{ex}} \sqrt{\frac{E^{ex}}{2E_k E_k^{ph}[4(E_k^{ex})^3 - E_k^{ex}E_k^2 + 4A_k^2 E_k^{ph}]}} \\
R_2 &= \frac{A_k(2E_k^{ex} - E_k)}{E_k^{ex}} \sqrt{\frac{2E_k^{ex}E_k^{ph}}{E_k[4(E_k^{ex})^3 - E_k^{ex}E_k^2 + 4A_k^2 E_k^{ph}]}} \\
R_3 &= \frac{(E_k + 2E_k^{ph})(4(E_k^{ex})^2 - E_k^2)}{4E_k^{ex}} \sqrt{\frac{E^{ex}}{2E_k E_k^{ph}[4(E_k^{ex})^3 - E_k^{ex}E_k^2 + 4A_k^2 E_k^{ph}]}} \\
R_4 &= \frac{A_k(2E_k^{ex} + E_k)}{E_k^{ex}} \sqrt{\frac{2E_k^{ex}E_k^{ph}}{E_k[4(E_k^{ex})^3 - E_k^{ex}E_k^2 + 4A_k^2 E_k^{ph}]}}
\end{aligned} \quad (4.16)$$

We calculate the dispersion curve according to Eq.(4.14) with the following parameter: cavity length $L_c = 0.252\mu m$, the thickness of QW $\Lambda = 100$Å. The result is illustrated in Fig 4.1. Both HH and HL case are considered. We also add in the figure the dispersion of bare photon and exciton for comparison. The anti-crossing behaviour of the upper and lower branches is obvious. We note that the dispersion of cavity photon is more like a parabola because

$$E_k^{ph} = \frac{1}{2}\hbar c\sqrt{(\frac{\pi}{L_c})^2 + k^2} \approx \frac{1}{2}(c\frac{\pi}{L_c} + \frac{\hbar^2 k^2}{2m_{eff}}) \quad (4.17)$$

$m_{eff} = \frac{\pi\hbar^2}{cL_c}$ is the "effective mass" of photon which results from the confinement of light in the cavity.

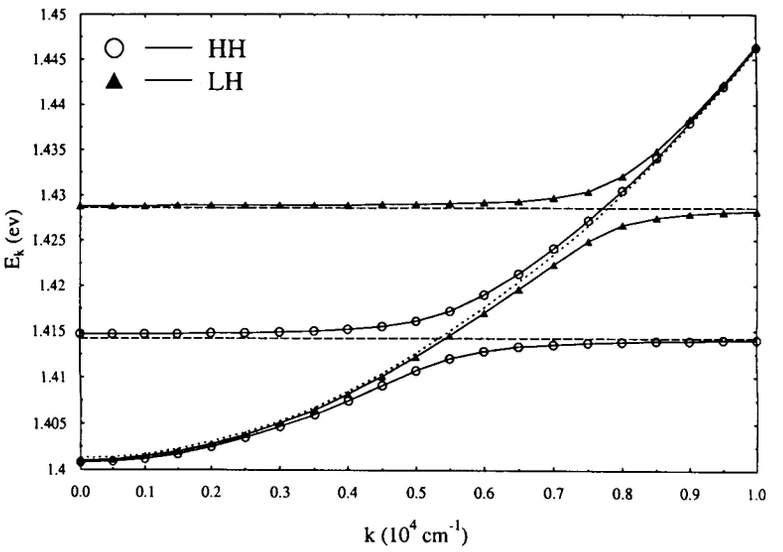

Figure 4.1: The dispersion curve of HH and LH exciton polariton in SMC

When the dissipation of light and exciton are both consiered, after solving the motion equation of photon and exciton fileds integratedly, we found the eigen frequency of the two branches around the resonance point:

$$\Omega_{k,\pm} = \frac{1}{\hbar}\Big(E_k^{ex} + E_k^{ph} - i(\Gamma_k^{ph} + \Gamma_k^{ex})/2 \pm \sqrt{[E_k^{ex} - E_k^{ph} - i(\Gamma_k^{ph} - \Gamma_k^{ex})/2]^2 + 4A_k}\Big) \quad (4.18)$$

So the polariton has the total linewidth of $\frac{\gamma_k^{ph}+\gamma_k^{ex}}{2}$ that is usually much smaller than the bare exciton linewidth. It demonstrates the extended property of polariton. Therefore, the disorder potential has the less influence on the polariton which is an advantage of using polaritons to explore the microcavity.

From (4.9) and (4.11), we have

$$\begin{aligned}\eta_k &= \cos\theta_k(a_k \cosh r + a_{-k}^{\dagger} e^{2i\varphi} \sinh r) + i \sin\theta_k(b_k \cosh r + b_{-k}^{\dagger} e^{2i(\varphi+\frac{\pi}{2})} \sinh r) \\ \eta_{-k} &= \cos\theta_k(a_{-k} \cosh r + a_k^{\dagger} e^{2i\varphi} \sinh r) + i \sin\theta_k(b_{-k} \cosh r + b_k^{\dagger} e^{2i(\varphi+\frac{\pi}{2})} \sinh r) \end{aligned} \quad (4.19)$$

So compared with (4.9) which are polariton operators when no squeezing is presented, (4.19) suggests the two steps of polariton squeezing: first, photon and exciton are squeezed respectively to the same degree, but the squeezing angles of the two components are out of phase;

then two squeezed components are mixed together to constitute a polariton. Because the squeezing is completely resulted from the doulbe-photon terms of interaction, it is essentially different from the squeezing in some nonlinear optical methods such as parametric amplification and bistablity. We call such kind of squeezing "intrinsic squeezing".

The squeezing angle is also determined by the intrinsic coupling between exciton and light. On resonance it gives

$$R_3^2 = R_1^2 e^{-2i\varphi} + 1 \tag{4.20}$$

Noting that R_3^2 and R_1^2 contain γ_k^{ex} and γ_k^{ph}, we find that the squeezing angle bear the information of dissipation. It provides another way to measure the dissipation of cavity and exciton: homodyne. By tuning the phase of local oscillator, we can observe the maxium squeezing at a certain value. Then we can calculate the total loss of polariton according to this phase value.

Two quadrature operators can be defined as:

$$\begin{aligned} X_k^q &= (c_k + c_{-k})e^{-i\varphi} + (c_k^\dagger + c_{-k}^\dagger)e^{i\varphi} \\ &= \cos\theta_k(q_k^{ph} + q_{-k}^{ph})e^{-i\varphi} - \sin\theta_k(p_k^{ex} + p_{-k}^{ex})e^{i\varphi} \end{aligned} \tag{4.21}$$

$$\begin{aligned} X_k^p &= -i[(c_k + c_{-k})e^{-i\varphi} - (c_k^\dagger + c_{-k}^\dagger)e^{i\varphi}] \\ &= \cos\theta_k(p_k^{ph} + p_{-k}^{ph})e^{-i\varphi} + \sin\theta_k(q_k^{ex} + q_{-k}^{ex})e^{i\varphi} \end{aligned} \tag{4.22}$$

which are canonical position and momentum operators. It is straightfoward to show that

$$SX_k^q S^\dagger = X_k^q e^{-r} \tag{4.23}$$

$$SX_k^p S^\dagger = X_k^p e^{r} \tag{4.24}$$

Polariton coherent states are the eigenstates of c_k and c_{-k}. We denote them as $|\alpha_k\rangle$ and $|\alpha_{-k}\rangle$. The squeezed states are obtained when S is operated on $|\alpha_{\pm k}\rangle$:

$$\begin{aligned} S|\alpha_k\rangle &= |\beta_k\rangle \\ S|\alpha_{-k}\rangle &= |\beta_{-k}\rangle \end{aligned} \tag{4.25}$$

The variance of X_k^q and X_k^p in the squeezed state are found to be:

$$\langle\beta_k|(\Delta X_k^q)^2|\beta_k\rangle = e^{-2r} \tag{4.26}$$

$$\langle\beta_k|(\Delta X_k^p)^2|\beta_k\rangle = e^{2r} \tag{4.27}$$

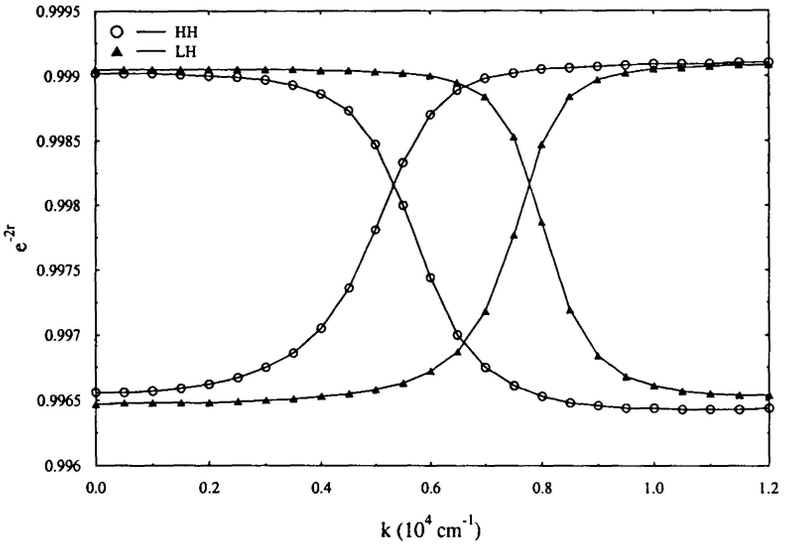

Figure 4.2: The squeezing degree of both branches of polariton in SMC; HH and LH considered

Considering that both quadratures in coherent state have the variance of 1, it is clear that the noise of one quadrature is squeezed while the other one is enhanced. We plot the squeezing degree as a function of in-plane wave-vector in Fig. 4.2. The squeezing degree of one branch increases with the momentum while the contrary holds for the other branch. It is not difficult to explain: when k is very small, the upper branch is exciton-like and the lower branch is photon-like. As k increases, the photon component in the upper branch is strengthened while the photon component in the lowered branch weakening. The squeezing effect is largely originated from the photon component because there is only double-photon term presented in the interaction Hamiltonian. When the density of exciton gets higher, we also expect the contribution from double-exciton term (a mean field approximation) or simply the exact four-exciton interaction [36]. Then the k dependence of squeezing will become more complicated. However, we leave it to later study.

Bibliography

[1] M. Born and K. Huang, Proc.R.Soc.London Ser.A **208**,352(1951)

[2] J.J. Hopfield, Phys. Rev. **112**, 1555(1958)

[3] C. Weisbuch, M. Nishioka, A. Ishikawa, and Y. Arakawa Phys. Rev. Lett. **69**, 3314-3317 (1992)

[4] R. Houdre, R. P. Stanley, U. Oesterle, M. Ilegems, and C. Weisbuch Phys. Rev. B **49**, 16761-16764 (1994)

[5] T. B. Norris, J.-K. Rhee, C.-Y. Sung, Y. Arakawa, M. Nishioka, and C. Weisbuch, Phys. Rev. B **50**, 14663 (1994)

[6] V. Savona, Z. Hradil, A. Quattropani, and P. Schwendimann Phys. Rev. B 49, 8774 (1994)

[7] J. Tignon, P. Voisin, C. Delalande, M. Voos, R. Houdre, U. Oesterle, and R. P. Stanley, Phys. Rev . Lett. **74**, 3967 (1995)

[8] T. B. Norris, J.-K. Rhee, C.-Y. Sung, Y. Arakawa, M. Nishioka, and C. Weisbuch Phys. Rev. B 50, 14663 (1994)

[9] A.V.Kavokin Phys. Rev. B **54**,1490 (1996)

[10] S. Pau, G. Björk, J. Jacobson, H. Cao, and Y. YamamotoPhys. Rev. B **51**, 7090 (1995)

[11] S. Pau, G. Björk, J. Jacobson, H. Cao, and Y. Yamamoto Phys. Rev. B 51, 14437(1995)

[12] A. Fainstein, B. Jusserand, and V. Thierry-Mieg Phys. Rev. Lett. **75**, 3764 (1995)

[13] Y. Chen, A. Tredicucci, and F. Bassani Phys. Rev. B 52, 1800 (1995)

[14] T. A. Fisher, A. M. Afshar, D. M. Whittaker, M. S. Skolnick, J. S. Roberts, G. Hill, and M. A. Pate, Phys. Rev. B **51**, 2600 (1995)

[15] G. Panzarini and L. C. Andreani, Phys. Rev. B 52, 10780 (1995)

[16] F. Tassone, C. Piermarocchi, V. Savona, A. Quattropani, and P. Schwendimann Phys. Rev. B **53**, R7642(1996)

[17] T. A. Fisher, A. M. Afshar, M. S. Skolnick, D. M. Whittaker, and J. S. Roberts Phys. Rev. B 53, R10469 (1996)

[18] V. Savona and C. Weisbuch Phys. Rev. B 54, 10835 (1996)

[19] M. R. Vladimirova, A. V. Kavokin, and M. A. Kaliteevski Phys. Rev. B **54**, 14566 (1996)

[20] R. P. Stanley, R. Houdre, C. Weisbuch, U. Oesterle, and M. Ilegems Phys. Rev. B 53, 10995 (1996)

[21] Y.Zhu et. al. Phys. Rev. Lett. **64**,2499(1990)

[22] F.Tasson, F. Bassani and L.C.Andreani, Il Nuovo Cimento 12,1673(1990)

[23] L.J.Sham ,2nd Inter. Conf. on MSS-II(japan) 573(1985)

[24] J. N. Shulman and Y. C. Chang, Phys. Rev. B **31**, 2056(1985)

[25] Bangfeng Zhu and Huang K., Phys. Rev. B **36**,8102(1988)

[26] Bangfeng Zhu, Phys. Rev. B **37**,4687(1988)

[27] L. Viña, R.T. Collins,F.E.Mendez, And W.I.Wang,Phys.Rev.Lett.**58**,832(1987); R.T. Collins,L. Viña,W.I.Wang,L.L.Chang, L. Esaki,K. v.Klitzing and K.Ploog,Phys. Rev. B **36**,1531(1987)

[28] Ansheng Liu, Phys. Rev. B **50**,8569(1994),*ibd* **55**,7101(1994)

[29] A.Yariv,Optical Waves in Crystal: Propagation and Control of the Laser Radiation, Wiley,New York(1984)

[30] O. Keller, Phys. Rev. B **37**,10588(1988)

[31] J.M.Luttinger,W.Kohn,Phys. Rev. **97**,869(1954)

[32] Hui Tang and Kun Huang ,Journal of Semiconductors,**8**,1(1987) (in Chinese),see also E.I Ivchenko and G.E.Pikus,Superlatices and other Heterostures,Springer-Verlag(1994)

[33] L. Andreani and A. Pasquarello, Phys. Rev. B **42**,8828(1990)

[34] G.D.Mahan, Many Particle Physics,2nd edition,Plenum,New York(1990)

[35] M.Artoni, J.L.Birman, Quantum Optics **1**, 91-97(1989)

[36] T.Hiroshima, Phys.Rev.B **40**,3862(1989);J.Phys.Condens Matter **4**,3849(1992)